AWARD NUMBER: W81XWH-19-1-0031

TITLE: Notch3 as a Tumor Suppressor in the Postpartum Mammary Gland

PRINCIPAL INVESTIGATOR: Keli Xu

CONTRACTING ORGANIZATION: University of Mississippi Medical Center

REPORT DATE: MAY 2023

TYPE OF REPORT: Annual

PREPARED FOR: U.S. Army Medical Research and Development Command
Fort Detrick, Maryland 21702-5012

REPORT DOCUMENTATION PAGE

Form Approved
OMB No. 0704-0188

1. REPORT DATE	2. REPORT TYPE	3. DATES COVERED
MAY 2023	Annual	1APR2022 - 31MAR2023

4. TITLE AND SUBTITLE

Notch3 as a Tumor Suppressor in the Postpartum Mammary Gland

5a. CONTRACT NUMBER

5b. GRANT NUMBER
W81XWH-19-1-0031

5c. PROGRAM ELEMENT NUMBER

6. AUTHOR(S)
Keli Xu

E-Mail: kxu@umc.edu

5d. PROJECT NUMBER

5e. TASK NUMBER

5f. WORK UNIT NUMBER

7. PERFORMING ORGANIZATION NAME(S) AND ADDRESS(ES)

University of Mississippi
Medical Center
2500 North State Street
Jackson, MS 39216

8. PERFORMING ORGANIZATION REPORT NUMBER

9. SPONSORING / MONITORING AGENCY NAME(S) AND ADDRESS(ES)

U.S. Army Medical Research and Development Command
Fort Detrick, Maryland 21702-5012

10. SPONSOR/MONITOR'S ACRONYM(S)

11. SPONSOR/MONITOR'S REPORT NUMBER(S)

12. DISTRIBUTION / AVAILABILITY STATEMENT

Approved for Public Release; Distribution Unlimited

13. SUPPLEMENTARY NOTES

14. ABSTRACT

We recently reported a tumor-suppressive function for Notch3 in the parous mammary gland through the restriction of parity-identified mammary epithelial cell (PI-MEC) expansion. Unexpectedly, syngeneic transplantation experiments revealed that the post-lactational involuting mammary microenvironment of Notch3 knockout (*Notch3*$^{-/-}$) mice suppressed tumor growth compared to that of wildtype mice. Moreover, non-parous mammary microenvironment of *Notch3*$^{-/-}$ mice also exhibited anti-tumor activity, and the tumor-suppressive effect was observed even when breast cancer cells were ectopically transplanted to a posterior dorsolateral site. To test whether suppression of tumor growth in *Notch3*$^{-/-}$ hosts is mediated through immune cells, we performed co-culture of breast cancer cells with splenocytes isolated from mice following tumor cell inoculation. Indeed, splenocytes from *Notch3*$^{-/-}$, but not wildtype, mice showed potent cytotoxicity against cancer cells. Thus, contrary to its tumor-suppressive function in the postpartum mammary epithelium, Notch3 may facilitate tumor development through the repression of anti-tumor immunity in tumor microenvironment. We are currently studying the mechanisms underlying the Notch3 modulation of anti-tumor immunity.

15. SUBJECT TERMS

Breast cancer, Notch signaling, Parity-identified mammary epithelial cell (PI-MEC), Tumor immune microenvironment, Anti-tumor immunity, Lipid metabolism.

16. SECURITY CLASSIFICATION OF:			17. LIMITATION OF ABSTRACT	18. NUMBER OF PAGES	19a. NAME OF RESPONSIBLE PERSON
a. REPORT	b. ABSTRACT	c. THIS PAGE			USAMRDC
U	U	U	UU	25	19b. TELEPHONE NUMBER *(include area code)*

Standard Form 298 (Rev. 8-98)
Prescribed by ANSI Std. Z39.18

TABLE OF CONTENTS

1. **INTRODUCTION:**

We propose to test the hypothesis that Notch3 functions as a tumor suppressor in the postpartum mammary gland by restricting the parity-associated mammary stem and progenitor-like cells, and by promoting brown adipocyte differentiation during post-lactational involution, which may ameliorate the pro-tumorigenic microenvironment. The specific aims of this project are: (1) determine whether the post-lactational involuting mammary microenvironment of Notch3 knockout mice accelerates tumor growth and metastasis compared to that of wild-type mice and whether Notch3 functions in the mammary epithelium or the stroma in this context; (2) determine the regulation of parity-identified mammary epithelial cells or other stem/progenitor populations by Notch3 in the postpartum mammary gland; (3) determine how Notch3 regulates brown adipocyte differentiation during involution and whether brown adipocytes have an impact on the postpartum mammary microenvironment. Our objectives are to: (1) determine the contribution of parity-identified mammary epithelial progenitors to postpartum breast cancer and its regulation by Notch signaling; (2) determine the mechanism underlying brown adipose tissue repopulation in the postpartum mammary gland and its potential role in modulating postpartum mammary microenvironment, which may link obesity-associated metabolic changes to the progression of postpartum breast cancer.

2. **KEYWORDS:**

Breast cancer, Notch signaling, Parity-identified mammary epithelial cell (PI-MEC), Tumor immune microenvironment, Anti-tumor immunity, Lipid metabolism.

3. **ACCOMPLISHMENTS:**

- **What were the major goals of the project?**

  Major Task 1: Determine whether post-lactational involuting mammary microenvironment of Notch3 knockout mice accelerates tumor growth and metastasis compared to that of wildtype mice.
  Milestone/target date: 01/31/2020
  Actual completion date: 12/01/2019

  Major Task 2: Determine the compartment in which Notch3 regulates pro-tumorigenic mammary microenvironment.
  Milestone/target date: 09/30/2020
  Actual completion date: 11/30/2020

  Major Task 3: Determine the mechanisms by which Notch3 regulates brown adipocyte differentiation in the involuting mammary gland.
  Milestone/target date: 04/30/2021
  Actual completion date: 04/12/2021

  Major Task 4: Determine whether brown adipocytes have an impact on pro-tumorigenic microenvironment in the postpartum mammary gland.
  Milestone/target date: 12/31/2021
  Ongoing (80% completion)

  Major Task 5: Determine alterations in the self-renewal and/or differentiation of PI-MECs or other stem/progenitor populations in parous Notch3 knockout mice.
  Milestone/target date: 03/31/2022
  Actual completion date: 02/15/2022

- **What was accomplished under these goals?**

Major activities:

1) Performed histological examination of mammary tumors from wild-type and Notch3 knockout mice following syngeneic transplantation of basal-like (B5725) and claudin-low (C0321) breast cancer cells, with a focus on the tumor-infiltrating lymphocytes.

2) Performed in vitro cytotoxicity tests for splenocytes and thymocytes isolated from wild-type and Notch3 knockout mice with or without injection of breast cancer cells. Briefly, B5725 and C0321 breast cancer cells were co-cultured with splenocytes or thymocytes isolated from host mice with injection of the respective cancer cells (suspended in DMEM medium mixed with Matrigel) or sham injection of DMEM/Matrigel only. Immune cell cytotoxicity was determined by measuring live cancer cells by MTT assay after 7 to 10 days of co-culture.

3) Performed expression analysis for Notch3 in the mouse spleen and determined alteration in B cell follicles in the Notch3 knockout mice. X-gal staining (as a surrogate for Notch3 expression) was performed in the spleen of wildtype (as negative control), *Notch3*$^{\beta\text{-}Geo/+}$ and *Notch3* $^{\beta\text{-}Geo/\beta\text{-}Geo}$ mice at 2 weeks post cancer cell injection.

4) Identified candidate genes downstream of Notch3 in the regulation of anti-tumor immunity. RNA-seq and differential gene expression analyses were performed in splenocytes isolated from the wild-type and Notch3 knockout mice following the injection of breast cancer cells.

Specific objectives:

Specific objective in this reporting period is to determine the roles of Notch3 in the mammary tumor immune microenvironment, and to determine whether Notch3 regulates anti-tumor immunity in part through the modulation of lipid metabolism.

Significant results:

1) We found that mammary tumor transplants in the Notch3 knockout mice contained abundant tumor-infiltrating lymphocytes (TILs), sometimes forming tertiary lymphoid structures (TLSs). To the contrary, mammary tumor transplants in the wild-type mice showed very few TILs (Fig. 1). These results suggest that Notch3 may function in the host immune system to regulate the recruitment, maturation, or activation of immune cells that suppress tumor growth.

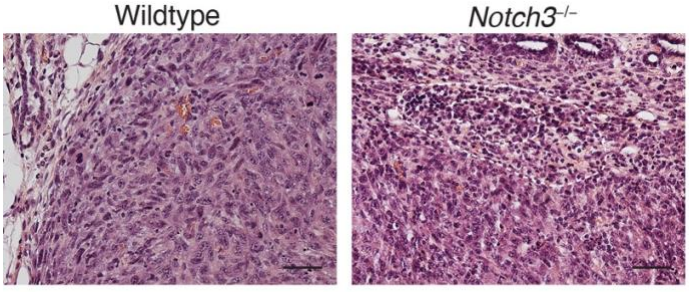

Fig. 1. Abundant tumor-infiltrating lymphocytes (TILs) in the Notch3 knockout mice but very few in wild-type mice following the transplantation of breast cancer cells.
Shown are representative histology of mammary tumors with adjacent normal tissues. Area circled with dotted line: TILs forming a tertiary lymphoid structure (TLS). Scale bar: 50 μm.

2) We discovered that splenocytes isolated from Notch3 knockout mice (following cancer cell injection) showed potent anti-cancer cell cytotoxicity, whereas splenocytes isolated from the wildtype mice (following cancer cell injection) showed little or no cytotoxic effect (Fig. 2A, B). Splenocytes isolated from Notch3 knockout mice with sham injection had no cytotoxic effect (Fig. 2C, D). In contrast to the splenocytes, thymocytes (naïve T cells) isolated from host mice showed no cytotoxicity (Fig. 2E, F). These results suggest that Notch3 may exert a tumor-promotive role in the host immune system through negative regulation of anti-tumor immunity.

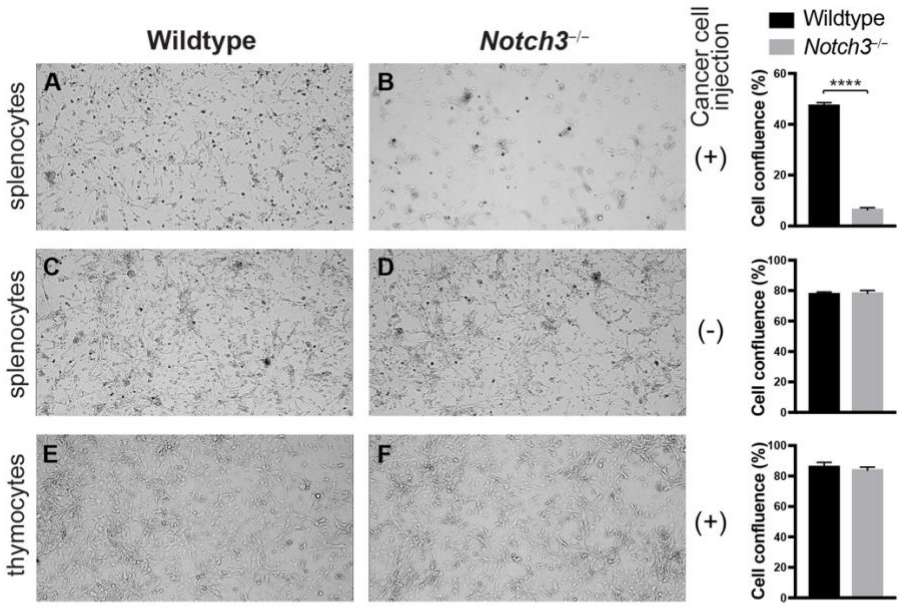

Fig. 2. Splenocytes isolated from the Notch3 knockout hosts exhibited potent cytotoxicity against cancer cells in vitro. Shown are representative images and quantitation of B5725 cells after nine days of co-culture with splenocytes (or thymocytes) isolated from wildtype or Notch3 knockout mice at two weeks post injection of B5725 cells or sham injection. **** $p<0.0001$.

3) We found that Notch3 is expressed in a limited number of splenocytes accumulating at the border between the T cell zone and B cell follicle (Fig. 3A), suggesting a potential role for Notch3 in the interaction between T and B lymphocytes. Moreover, Notch3 knockout mice contained significantly increased number of secondary B follicles (i.e., containing a germinal center) as compared to the wild-type mice (Fig. 3B), hinting a potential role for Notch3 in the regulation of B cell responses to tumor cells.

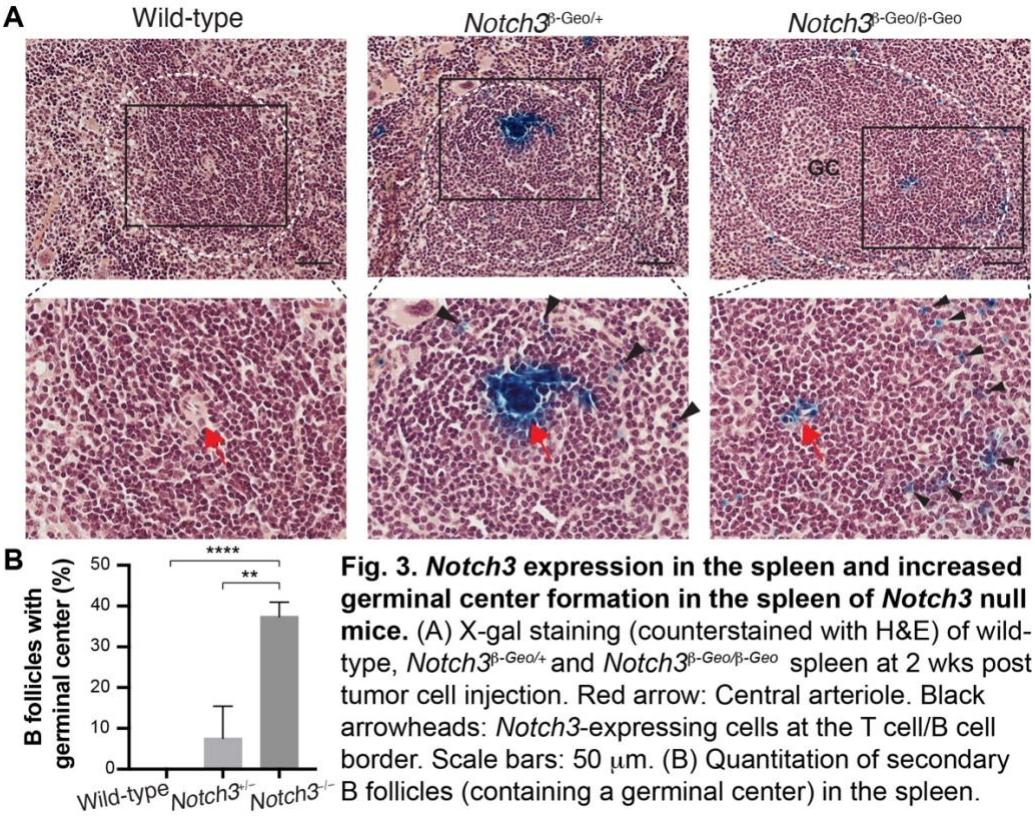

Fig. 3. *Notch3* expression in the spleen and increased germinal center formation in the spleen of *Notch3* null mice. (A) X-gal staining (counterstained with H&E) of wild-type, *Notch3*$^{β\text{-}Geo/+}$ and *Notch3*$^{β\text{-}Geo/β\text{-}Geo}$ spleen at 2 wks post tumor cell injection. Red arrow: Central arteriole. Black arrowheads: *Notch3*-expressing cells at the T cell/B cell border. Scale bars: 50 μm. (B) Quantitation of secondary B follicles (containing a germinal center) in the spleen.

4) In corroboration with increased number of germinal centers (GCs), Notch3-deficient splenocytes showed higher expression of Uchl1, a gene specifically expressed in GC B cells. Moreover, Notch3-deficient splenocytes showed upregulation of many of the immunoglobulin genes and major histocompatibility complex class II (MHCII) genes (6 out of 13 top upregulated genes, Table 1), suggesting enhanced antibody production and antigen presentation by B cells. It has recently been shown that follicular regulatory T (Tfr) cells express decoy IL-1R2 receptor to suppress IL-1-mediated activation of follicular helper T (Tfh) cells, thereby restricting Tfh-dependent B cell activation. Like Notch3-expressing cells, Tfr cells were previously shown to convene at the border between the T cell zone and B cell follicle. We found downregulation of IL-1R2 in Notch3 knockout splenocytes (Table 1), suggesting that Notch3 may upregulate IL-1R2 expression in Tfr cells.

5) RNA-seq analysis revealed downregulation of lipid metabolism genes, Fabp5 and Dgat2, in the Notch3-deficient splenocytes (Table 1). Intriguingly, previous study found that IL-1R2 expression was reduced in monocytes from patients with familial combined hyperlipidemia, and macrophages incubated with acetylated low density and very low density lipoproteins also exhibited a decrease in IL-1R2 level, whereas pre-incubation with agents that block intracellular lipid accumulation prevented the decrease in IL-1R2. Expression of IL1R2 is positively correlated to FABP5 and DGAT2 expressions in human breast cancer (Fig. 4), and high expression of FABP5 and DGAT2 are both associated with poor relapse-free survival (Fig. 5). These findings suggest that Notch3 may regulate anti-tumor immunity in part through the modulation of Fabp5, Dgat2-mediated lipid metabolism.

Table 1. Top differentially expressed genes in *Notch3*$^{-/-}$ splenocytes

log2 fold change	p value	p adjust	Gene name
	Upregulated		
4.34198006	2.29E-15	1.13E-11	H2-Eb1
2.80789495	1.42E-07	0.00026176	H2-Aa
3.24645419	4.73E-07	0.0006342	Btnl6
1.54823358	3.80E-06	0.00267034	Igkv3-10
1.58756851	6.01E-06	0.0034123	Vars
2.44048595	3.39E-05	0.00939282	H2-Q10
2.15266383	3.89E-05	0.01008269	H2-Ab1
1.83534775	5.21E-05	0.01110731	H2-K1
1.7928536	0.00031874	0.03311729	Gm20506
1.76772865	0.00047732	0.04248076	Vwa7
1.67071991	0.00056657	0.04592973	Iigp1
1.8282002	0.00063965	0.04794061	Nccrp1
1.7851485	0.00066694	0.04894513	Gm37614
	Downregulated		
-6.8114905	1.79E-30	2.65E-26	H2-Ea-ps
-3.1318155	8.47E-24	6.25E-20	Gm11361
-4.9563314	5.97E-15	2.20E-11	Gm4134
-3.1278281	4.07E-09	1.20E-05	Vcan
-2.5899127	3.77E-08	9.28E-05	Prtn3
-3.2819379	5.17E-08	0.00010895	BC100530
-3.2108197	3.07E-07	0.00046281	Adamtsl5
-2.2170232	3.14E-07	0.00046281	Gm17383
-2.7611204	7.08E-07	0.00087007	Chil3
-2.3879759	1.04E-06	0.00118362	Elane
-2.0902752	1.78E-06	0.00188099	Ms4a3
-3.1704357	2.13E-06	0.0020988	Gpr150
-2.5711231	2.44E-06	0.00211919	F10
-2.6907784	2.36E-06	0.00211919	Crispld2
-2.2383529	2.85E-06	0.00221325	Ctsg
-2.9615552	2.85E-06	0.00221325	Gm6166
-2.7473397	3.56E-06	0.00262547	Il1r2
-3.0333838	4.11E-06	0.00275311	Plek2
-2.1755594	4.48E-06	0.00287528	Lrg1
-2.7757849	4.85E-06	0.00296822	Fabp5
-2.2892826	5.03E-06	0.00296822	Mpo
-2.0005816	7.69E-06	0.00420207	Dgat2

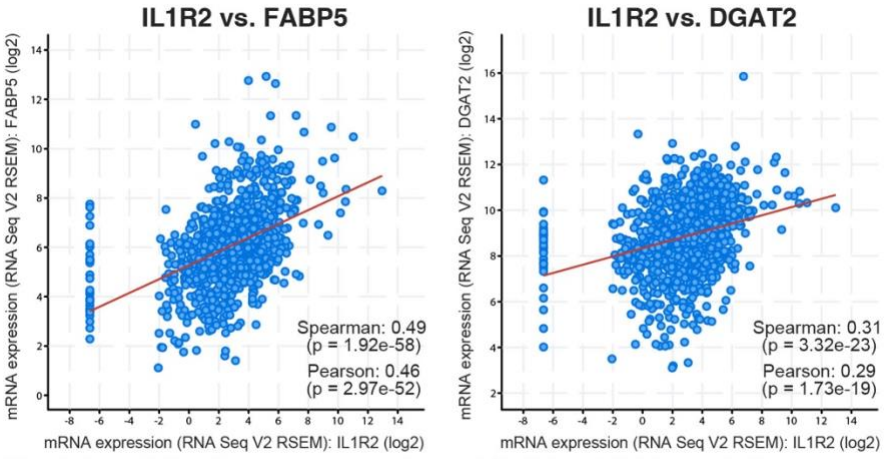

Fig. 4. Correlation between expressions of *IL1R2* and lipid metabolism genes *FABP5* and *DGAT2* in human breast cancer (TCGA dataset hosted in cBioPortal).

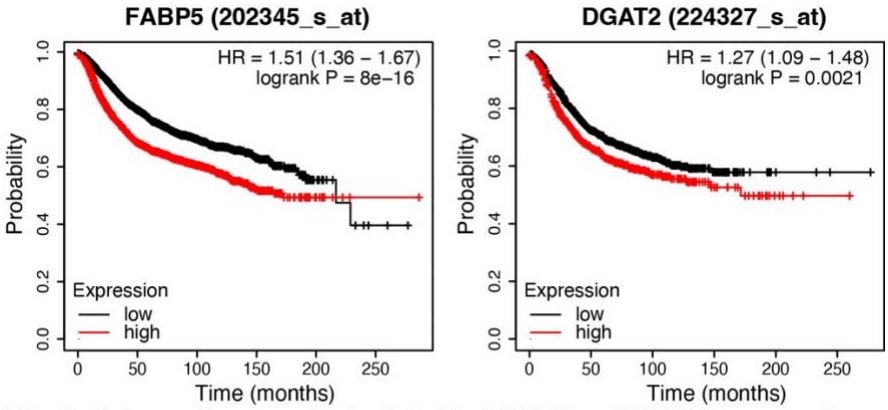

Fig. 5. Relapse-free survival related to FABP5 and DGAT2 expression in breast cancer of all subtypes (derived from http://www.kmplot.com).

Discussion of stated goals not met:

We were not able to complete the Major Task 4, "determine whether brown adipocytes have an impact on pro-tumorigenic microenvironment in the postpartum mammary gland", as originally planned. We hypothesized that Notch3 might regulate transdifferentiation of alveolar myoepithelial cell to brown adipocyte during post-weaning involution. Our results and studies by others indicate that very few brown adipocytes are converted from mammary epithelial cells in the post-weaning mammary gland, and that Notch3 regulates brown adipocyte differentiation in the stroma. Defective brown adipocyte differentiation in the Notch3 knockout mice during post-weaning involution may contribute to the expansion of stem-like PI-MECs (Chung et al., 2022). However, the number of brown adipocytes decreases dramatically after the first phase of post-weaning involution, it is thus unlikely that brown adipocytes have a significant impact in the postpartum mammary gland. Intriguingly, Notch3-deficient splenocytes showed down-regulation of lipid metabolism genes, suggesting that Notch3 may regulate lipid metabolism in immune cells. We are currently testing this hypothesis.

- **What opportunities for training and professional development has the project provided?**

  Nothing to report.

- **How were the results disseminated to communities of interest?**

  This project was highlighted in the Annual Report of the Cancer Center and Research Institute at the University of Mississippi Medical Center that reaches to the local community. A research paper resulting from this project was recently published in *Development*, accompanied by a "Research Highlight" that unpacks the findings of the paper and is accessible to all readers within the developmental biology community.

- **What do you plan to do during the next reporting period to accomplish the goals?**

  We plan to determine roles of Fabp5 and Dgat2 in the regulation of IL-1R2 expression as well as anti-tumor immunity. We will treat human Treg cell line with Fabp5 and Dgat2 inhibitors to test the effect on IL-1R2 expression. We will test the anti-tumor efficacy of Fabp5 and Dgat2 inhibitors using co-culture of cancer cells with splenocytes isolated from wildtype mice. Fabp5 may regulate lipid quality/quantity to promote cancer cell growth and survival and Dgat2 inhibition was recently shown to impair lipid biosynthesis and sensitize breast cancer cells to radiation. Therefore, we will test whether inhibitors have a direct effect on cancer cells. If they do, we will pretreat splenocytes with the inhibitors for the coculture experiment to determine the immune cell-mediated effects. Finally, we will test the anti-tumor efficacy of pharmacological inhibition of Fabp5 and Dgat2 in syngeneic transplantation breast cancer model.

4. **IMPACT:**

- **What was the impact on the development of the principal discipline(s) of the project?**

  Previously neglected, B lymphocytes are now considered key cellular components that initiate and sustain anti-tumor responses and are indispensable allies of T lymphocyte in eliminating cancer cells. Our preliminary data suggest that deletion of Notch3 may downregulate IL-1R2 in Tfr cells thereby enhancing IL-1-mediated Tfh stimulation, leading to increased B cell anti-tumor responses. Notch3 may regulate IL-1R2 and other immunoregulatory molecules through the modulation of Fabp5, Dgat2-mediated lipid metabolism, therefore Fabp5 and Dgat2 may represent new immunotherapeutic targets.

- **What was the impact on other disciplines?**

  Nothing to report.

- **What was the impact on technology transfer?**

  Nothing to report.

- **What was the impact on society beyond science and technology?**

  Nothing to report.

5. **CHANGES/PROBLEMS:**

- **Changes in approach and reasons for change**

  Nothing to report.

- **Actual or anticipated problems or delays and actions or plans to resolve them**

  Due to the COVID-19 pandemic, on-campus research activities at the University of Mississippi Medical Center ramped down in 2020. We also experienced delays and shortages of research materials in the past three years, which have had a negative impact on the progress of this project. During the past 12 months of 1st NCE period, significant progress has been made towards completion of the scope of work. However, the Major Task 4 "Determine whether brown adipocytes have an impact on pro-tumorigenic microenvironment in the postpartum mammary gland" is still not completed. For this reason, we requested and have been approved a 2nd NCE of 9 months to complete this project by December 31, 2023. We will complete the remaining work, specifically, determining the functions of two lipid metabolism genes identified in Major Task 4.

- **Changes that had a significant impact on expenditures**

  Nothing to report.

- **Significant changes in use or care of human subjects, vertebrate animals, biohazards, and/or select agents.**

  Nothing to report.

- **Significant changes in use or care of human subjects**

  N.A.

- **Significant changes in use or care of vertebrate animals**

No significant changes in use or care of vertebrate animals.

- **Significant changes in use of biohazards and/or select agents**

  No significant changes in use of biohazards and/or select agents.

6. **PRODUCTS:**

   - **Publications, conference papers, and presentations**

     - **Journal publications.**

       Chung W-C, Egan SE, Xu K. A tumor-suppressive function for Notch3 in the parous mammary gland. Development. 2022;149(19):dev200913. PMID: 36205077

       Acknowledgement of federal support: yes

     - **Books or other non-periodical, one-time publications.**

       Nothing to report.

     - **Other publications, conference papers, and presentations.**

       Nothing to report.

   - **Website(s) or other Internet site(s)**
     https://journals.biologists.com/dev/article/149/19/e149_e1905/277269/Notch3-protects-against-birth-associated-mammary

   - **Technologies or techniques**
     Nothing to report.

   - **Inventions, patent applications, and/or licenses**
     Nothing to report.

   - **Other Products**
     Nothing to report.

7. **PARTICIPANTS & OTHER COLLABORATING ORGANIZATIONS**

   - **What individuals have worked on the project?**

Name: Keli Xu (PI)	No change
Name: Wen-Cheng Chung (Scientist I)	No change

   - **Has there been a change in the active other support of the PD/PI(s) or senior/key personnel since the last reporting period?**

     Nothing to Report.

   - **What other organizations were involved as partners?**

     Nothing to Report.

8. **SPECIAL REPORTING REQUIREMENTS**

- **COLLABORATIVE AWARDS:** N.A.
- **QUAD CHARTS:** N.A.

9. **APPENDICES:**

A Research Article published in *Development* and a companion “Research Highlight”.

© 2022. Published by The Company of Biologists Ltd | Development (2022) 149, dev200913. doi:10.1242/dev.200913

RESEARCH ARTICLE

A tumor-suppressive function for Notch3 in the parous mammary gland

Wen-Cheng Chung[1], Sean E. Egan[2] and Keli Xu[1,3,*]

ABSTRACT

Notch3 promotes mammary luminal cell specification and forced Notch3 activation can induce mammary tumor formation. However, recent studies suggest a tumor-suppressive role for Notch3. Here, we report on Notch3 expression and functional analysis in the mouse mammary gland. Notch3 is expressed in the luminal compartment throughout mammary gland development, but switches to basal cells with initiation of post-lactational involution. Deletion of Notch3 caused a decrease of Notch activation in luminal cells and diminished luminal progenitors at puberty, as well as reduced alveolar progenitors during pregnancy. Parous *Notch3*$^{-/-}$ mammary glands developed hyperplasia with accumulation of CD24^{hi}CD49f^{lo} cells, some of which progressed to invasive tumors with luminal features. Notch3 deletion abolished Notch activation in basal cells during involution, accompanied by altered apoptosis and reduced brown adipocytes, leading to expansion of parity-identified mammary epithelial cells (PI-MECs). Interestingly, the postpartum microenvironment is required for the stem cell activity of *Notch3*$^{-/-}$ PI-MECs. Finally, high expression of NOTCH3 is associated with prolonged survival in patients with luminal breast cancer. These results highlight an unexpected tumor-suppressive function for Notch3 in the parous mammary gland through restriction of PI-MEC expansion.

KEY WORDS: Parity-identified mammary epithelial cell (PI-MEC), Notch3, Post-lactational involution, Mammary gland microenvironment, Brown adipocyte, Ucp1, Mouse

INTRODUCTION

Breast cancer is one of the most commonly diagnosed malignancies and a leading cause of cancer-related death among women worldwide. Epidemiological studies suggest that parity has a complex impact on the risk of breast cancer. Early full-term pregnancy reduces the lifetime risk, yet women also experience a transient increase in breast cancer risk that peaks approximately 5-6 years after giving birth and may persist for up to three decades (Albrektsen et al., 2005; Chie et al., 2000; Lambe et al., 1994; Liu et al., 2002). The paradoxically opposing effects of parity have been attributed to differentiation of mammary stem cells (MaSC) and the proliferation of precancerous cells, respectively, following pregnancy-associated hormonal changes (Polyak, 2006). Pregnancy also leads to a transient expansion of the MaSC compartment, likely mediated through paracrine signaling from RANK ligand (Asselin-Labat et al., 2010). In addition to the impact on the mammary epithelial cells, pregnancy, lactation and post-lactational involution profoundly alter the mammary stromal compartment, which may promote initiation and progression of postpartum breast cancer. The involuting mammary gland, which undergoes tissue remodeling with leukocyte infiltration and adipocyte repopulation, has been shown to accelerate tumor growth and metastasis (Guo et al., 2017; Lyons et al., 2014, 2011; Martinson et al., 2015; Schedin et al., 2007). Further understanding of parity-related alterations may lead to identification of preventative therapies for postpartum breast cancer.

A parous mammary gland is different from a nulliparous mammary gland, resulting in part from the formation of a new mammary epithelial cell population during pregnancy (Wagner et al., 2002). These parity-identified mammary epithelial cells (PI-MECs) are defined as a subset of pregnancy hormone-responsive cells that activate the promoter of late milk protein genes during pregnancy and lactation and bypass programmed cell death during post-lactational remodeling of the gland (Matulka et al., 2007). PI-MECs are able to proliferate and produce new secretory acini in subsequent pregnancies (Wagner et al., 2002). Virtually all PI-MECs express CD24, with the vast majority co-expressing CD49f (also known as Itga6), and a portion of PI-MECs are found within the MaSC-enriched CD24^{+}CD49f^{hi} mammary epithelial cell fraction (Matulka et al., 2007). Indeed, isolated PI-MECs were able to form mammospheres *in vitro*, generate both luminal and myoepithelial lineages to establish a fully functional mammary gland upon transplantation, and were able to self-renew over several transplant generations (Boulanger et al., 2005; Matulka et al., 2007). Interestingly, PI-MECs serve as targets of MMTV-neu/ErbB2-induced tumorigenesis (Henry et al., 2004; Jeselsohn et al., 2010).

Notch, a conserved signaling pathway, plays an important role in regulation of mammary epithelial differentiation and proliferation. *In vitro* studies using primitive cells from normal human mammary tissue showed activation of NOTCH3 to be essential for the restriction of bipotent progenitors to the luminal lineage (Raouf et al., 2008). In mice, Notch3 is expressed in a highly clonogenic and transiently quiescent luminal progenitor cell population that is capable of surviving multiple pregnancies. Also, Notch3 restricts the proliferation and consequent clonal expansion of these cells (Lafkas et al., 2013). Pregnant mice expressing an activated intracellular form of Notch3 (MMTV-Notch3^{ICD}) show expansion of a premalignant luminal progenitor population (Ling et al., 2013). Following parity, these mice develop luminal-subtype mammary tumors in a cyclin D1-dependent manner (Ling et al., 2013). Here, we used *Notch3*$^{\beta\text{-}geo}$ mutant mice to define its function in mammary epithelium. Consistent with its function in restricting expansion of PI-MECs, we identified a tumor-suppressive role for Notch3 in the postpartum mammary gland. In addition, we tested for NOTCH3

[1]Cancer Center and Research Institute, University of Mississippi Medical Center, Jackson, MS 39216, USA. [2]Program in Cell Biology, The Peter Gilgan Center for Research and Learning, The Hospital for Sick Children, Toronto, ON M5G 0A4, Canada. [3]Department of Cell and Molecular Biology, University of Mississippi Medical Center, Jackson, MS 39216, USA.

*Author for correspondence (kxu@umc.edu)

K.X., 0000-0001-5535-1076

Handling Editor: Liz Robertson
Received 5 May 2022; Accepted 1 September 2022

Development (2022) 149, dev200913. doi:10.1242/dev.200913

expression in association with survival in human breast cancer. The results corroborate our finding in mice that Notch3 suppresses luminal breast cancer.

RESULTS

Deletion of Notch3 caused decreased Notch-dependent transcription in luminal epithelium associated with reduced accumulation of luminal progenitors in the pubescent mammary gland

We used a *Notch3*$^{\beta\text{-}geo}$ knock-in allele, harboring a transmembrane-anchored *β-geo* fused in-frame with sequences coding for the first 21 EGF repeats of Notch3 (Xu et al., 2010), to define expression and functions of Notch3 in the mouse mammary gland. X-gal staining in pubescent *Notch3*$^{\beta\text{-}geo/+}$ mice showed robust expression in body cells of the terminal end buds (TEBs) and luminal cells of mature ducts (Fig. 1A). To determine alterations in Notch signaling associated with *Notch3* deletion, we crossed a Transgenic Notch Reporter (TNR), containing an eGFP expression cassette under the regulation of an artificial Notch-responsive promoter with multiple RBPJκ-binding sites (Duncan et al., 2005), into *Notch3*$^{\beta\text{-}geo/\beta\text{-}geo}$ (hereinafter referred to as *Notch3*$^{-/-}$) mice. Lineage-depleted mammary epithelial cells isolated from *TNR* and *Notch3*$^{-/-}$*;TNR* mice were stained for surface markers CD24, CD49f, CD61 (Itgb3) and Sca1 (Ly6a) to analyze Notch signaling in various epithelial subsets of the mammary gland. In *TNR* mice, GFP expression was detected in ∼10% of CD24^{+}CD49f^{hi} cells, a population known to contain MaSC (Stingl et al., 2006), and in nearly 30% of CD24^{hi}CD49f^{lo} cells, a population enriched for lobule progenitors (Jeselsohn et al., 2010). *Notch3*$^{-/-}$*;TNR* mice showed a reduced number of GFP^{+} cells, especially within the CD24^{hi}CD49f^{lo} population, suggesting that deletion of Notch3 causes decreased Notch-dependent transcription in lobule progenitors (Fig. 1B,C). The *Notch3*$^{-/-}$*;TNR* mutants also had a significantly reduced number of luminal progenitors (CD24^{hi}CD49f^{lo}CD61^{+}) (Asselin-Labat et al., 2007; Visvader and Stingl, 2014) compared with *TNR* mice (Fig. 1B,C). Of note, GFP expression was detected in ∼20% of the CD24^{hi}CD49f^{lo} cells in the *Notch3*$^{-/-}$*;TNR* mice, suggesting that other Notch receptors are still active in these cells. Therefore, Notch3 receptor may activate expression of a unique set of Notch target genes that are important for the luminal cell fate determination during mammary gland maturation. Anti-GFP immunostaining confirmed a reduced number of GFP-expressing cells within the TEB body cell compartment, as well as in luminal cells of mature ducts in *Notch3*$^{-/-}$*;TNR* mammary glands (Fig. 1D,E). Although Notch3 is expressed predominantly in the luminal cells, weak Notch3 expression is noted in a few basal cells. *Notch3*$^{-/-}$*;TNR* mice also showed a slightly decreased percentage of GFP^{+} cells in CD24^{+}CD49f^{hi} population (Fig. 1B) and a reduced number of GFP^{+} TEB cap cells (Fig. 1D), suggesting that Notch3 may be activated in a subset of basal cells. Interestingly, *Notch3* mutants exhibited increased keratin 14 (myoepithelial cell marker) expression in TEB cap cells but decreased keratin 8 (luminal cell marker) expression in mature ducts, suggesting skewed differentiation of bipotent progenitors towards myoepithelial lineage (Fig. 1F,H). However, ductal morphogenesis in these mice appeared to be indistinguishable from that seen in wild-type mice (Fig. 1G,I).

Notch3 deletion mice exhibit a reduced number of alveolar progenitors and show altered mammary alveolar morphogenesis during pregnancy

Notch3^{+} cells contribute to the formation of alveolar buds during pregnancy (Lafkas et al., 2013). Indeed, X-gal staining of *Notch3*$^{\beta\text{-}geo/+}$ mammary glands at pregnancy day 17.5 showed that Notch3 expression is high in alveolar cells but weak in ducts (Fig. S1A). Consistent with a role for Notch3 in this context, fewer CD24^{hi}CD49f^{lo}CD61^{+}Sca1^{-} cells, a population enriched for alveolar progenitors (Visvader and Stingl, 2014), were seen in *Notch3* mutants at mid-pregnancy (Fig. S1B). Also, whole-mount mammary gland preparation at late-pregnancy showed that *Notch3*$^{-/-}$ mutants had smaller alveoli compared with wild-type mice (Fig. S1C,D). Expressions of keratin 8 and 14 (luminal and myoepithelial markers, respectively) appeared to be normal in *Notch3* mutant glands (Fig. S1C). Thus, deletion of Notch3 had no effect on luminal versus myoepithelial cell fate specification during pregnancy; however, it did lead to a reduced number of alveolar progenitors with defective alveolar morphogenesis.

Deletion of Notch3 led to excess accumulation of PI-MECs accompanied by a decreased number of brown adipocytes

Despite the slight defect in alveolar morphogenesis during pregnancy, pups of *Notch3*$^{-/-}$ mice had similar size at weaning compared with pups from wild-type mice (Fig. S1E), suggesting normal lactation in *Notch3* mutants. *Notch3* expression remained high in mammary alveolar cells during lactation (Fig. 2A). Interestingly, forced weaning of pups at lactation day 10 caused a drastic downregulation of Notch3 in secretory alveolar cells (Fig. 2B,U). By post-weaning involution day 2, Notch3 expression was mostly restricted to myoepithelial cells (Fig. 2B). Expressions of the Notch ligands Jag1 and Dll1 were also detected in myoepithelial cells, and Jag1 expression was upregulated during involution (Fig. 2C-F,U). Consistent with the expression data, *TNR* mice displayed GFP^{+} myoepithelial cells at the onset of involution (Fig. 2G), whereas *Notch3*$^{-/-}$*;TNR* mice had no or very weak GFP expression at this stage (Fig. 2H,V), indicating that deletion of Notch3 abolished Notch signaling in myoepithelial cells of the involuting alveoli. Using whole-mount analysis, post-lactational involution appeared to proceed normally in *Notch3*$^{-/-}$ mice (Fig. S2). However, the number of TUNEL^{+} apoptotic cells was increased in mutant glands at involution day 1 but decreased at involution days 2 and 3 (Fig. 2I-N,W). In addition, *Notch3*$^{-/-}$ mammary glands showed a significantly increased number of p53^{+} alveolar cells compared with the wild type at involution day 1 (Fig. 2O,P,X). It has been shown that *p53* (*Trp53*) mRNA is upregulated at the start of involution (Strange et al., 1992), and that p53 participates in the first stage of involution initiated by the epithelium itself, but does not affect the second phase which involves stromal proteases (Jerry et al., 1998). These results suggest that deletion of Notch3 caused accelerated apoptosis at the start of involution but reduced cell death in the second phase of involution and remodeling. PI-MECs, a subset of alveolar cells that survive involution and post-lactation remodeling, exhibit stem cell characteristics and can serve as cellular targets for transformation (Henry et al., 2004; Matulka et al., 2007). Reduced cell death in the second phase of involution may lead to increased PI-MECs in *Notch3*$^{-/-}$ mice. We next analyzed PI-MEC levels by labeling mammary epithelium during pregnancy using *R26*^{YFP}*;WAP-Cre* and then by staining for YFP at involution day 28 post lactation. Indeed, *Notch3*$^{-/-}$*;R26*^{YFP}*;WAP-Cre* mice contained a significantly increased number of YFP^{+} cells compared with *R26*^{YFP}*;WAP-Cre* mice, suggesting that deletion of *Notch3* caused an increase in PI-MEC accumulation (Fig. 2Q,R,Y). Remodeling of the mammary gland during post-lactational involution is accompanied by adipocyte repopulation. Interestingly, brown adipocytes, which stain positive for Ucp1, emerged in close vicinity to alveolar

Development (2022) 149, dev200913. doi:10.1242/dev.200913

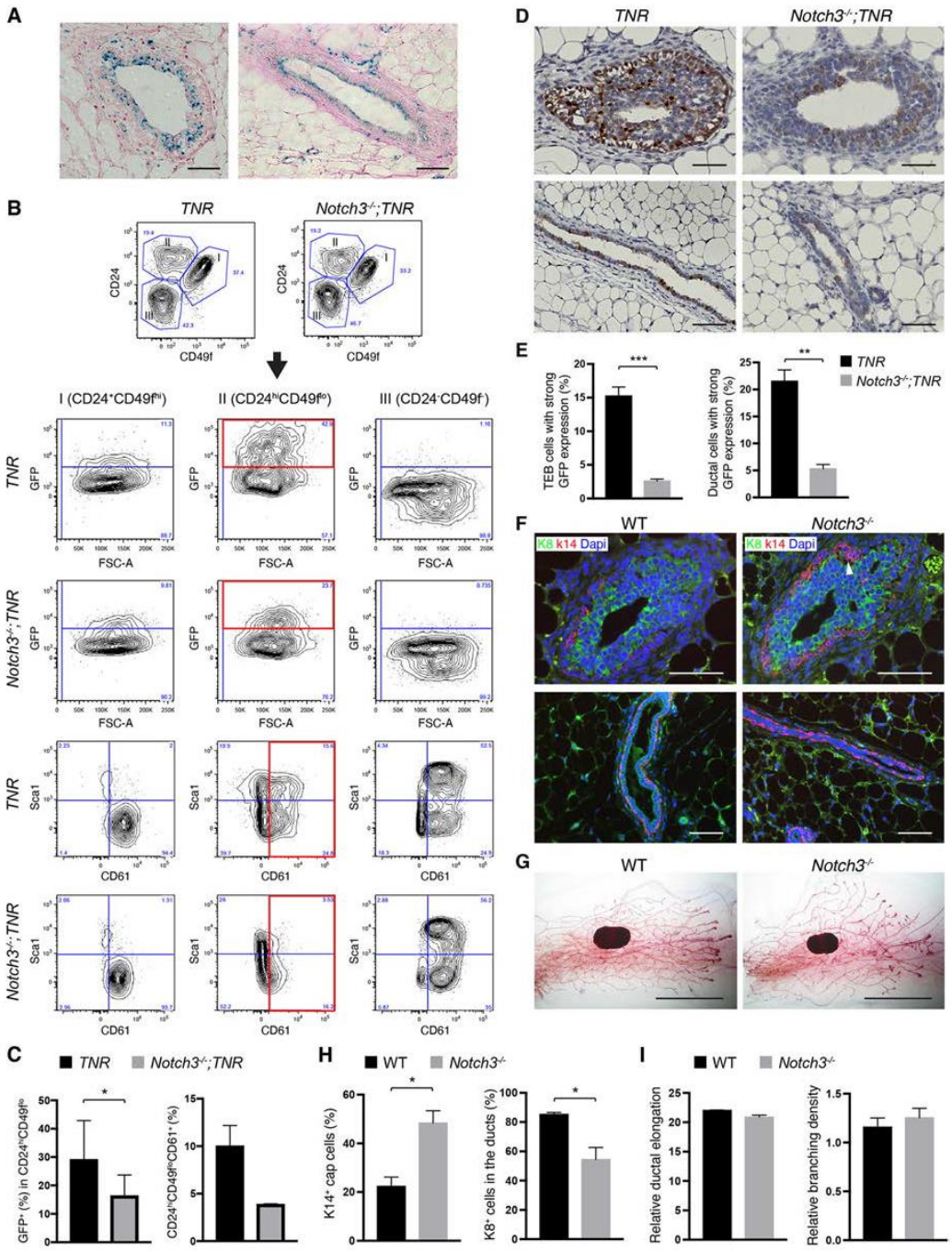

Fig. 1. The pubescent *Notch3*$^{-/-}$ mammary gland exhibits decreased Notch signaling in the luminal compartment associated with diminished CD24^{hi}CD49f^{lo}CD61^{+} luminal progenitors. (A) X-Gal staining of mammary tissue from a 6-week-old *Notch3*$^{\beta\text{-}geo/+}$ mouse showing the TEB (left) and mature duct (right). (B) Representative flow cytometry analysis of lineage-depleted mammary cells isolated from *TNR* and *Notch3*$^{-/-}$*;TNR* mice at 7-8 weeks of age. (C) Quantitation of GFP-positive cells in CD24^{hi}CD49f^{lo} population and comparison of the CD24^{hi}CD49f^{lo}CD61^{+} subpopulation. (D) Anti-GFP immunostaining in the TEBs (upper) and mature ducts (lower) of *TNR* and *Notch3*$^{-/-}$*;TNR* mice. (E) Percentage of TEB cells with strong GFP staining and percentage of ductal cells with strong GFP staining in *TNR* and *Notch3*$^{-/-}$*;TNR* mice. (F) Keratin 8 (K8) and keratin 14 (K14) immunofluorescence staining in the TEBs (upper) and mature ducts (lower) of wild-type and *Notch3*$^{-/-}$ mice. (G) Representative whole-mount mammary glands from 6-week-old wild-type and *Notch3*$^{-/-}$ virgins. (H) Percentage of K14^{+} cap cells and percentage of K8^{+} ductal cells in the wild-type and *Notch3*$^{-/-}$ mammary glands. (I) Relative length of ductal elongation and relative density of branching points in the wild-type and *Notch3*$^{-/-}$ mammary glands. Scale bars: 50 µm in A,D,F; 5 mm in G. Data are mean±s.e.m. **P*<0.05, ***P*<0.01, ****P*<0.001 (paired two-tailed Student's *t*-test).

Development (2022) 149, dev200913. doi:10.1242/dev.200913

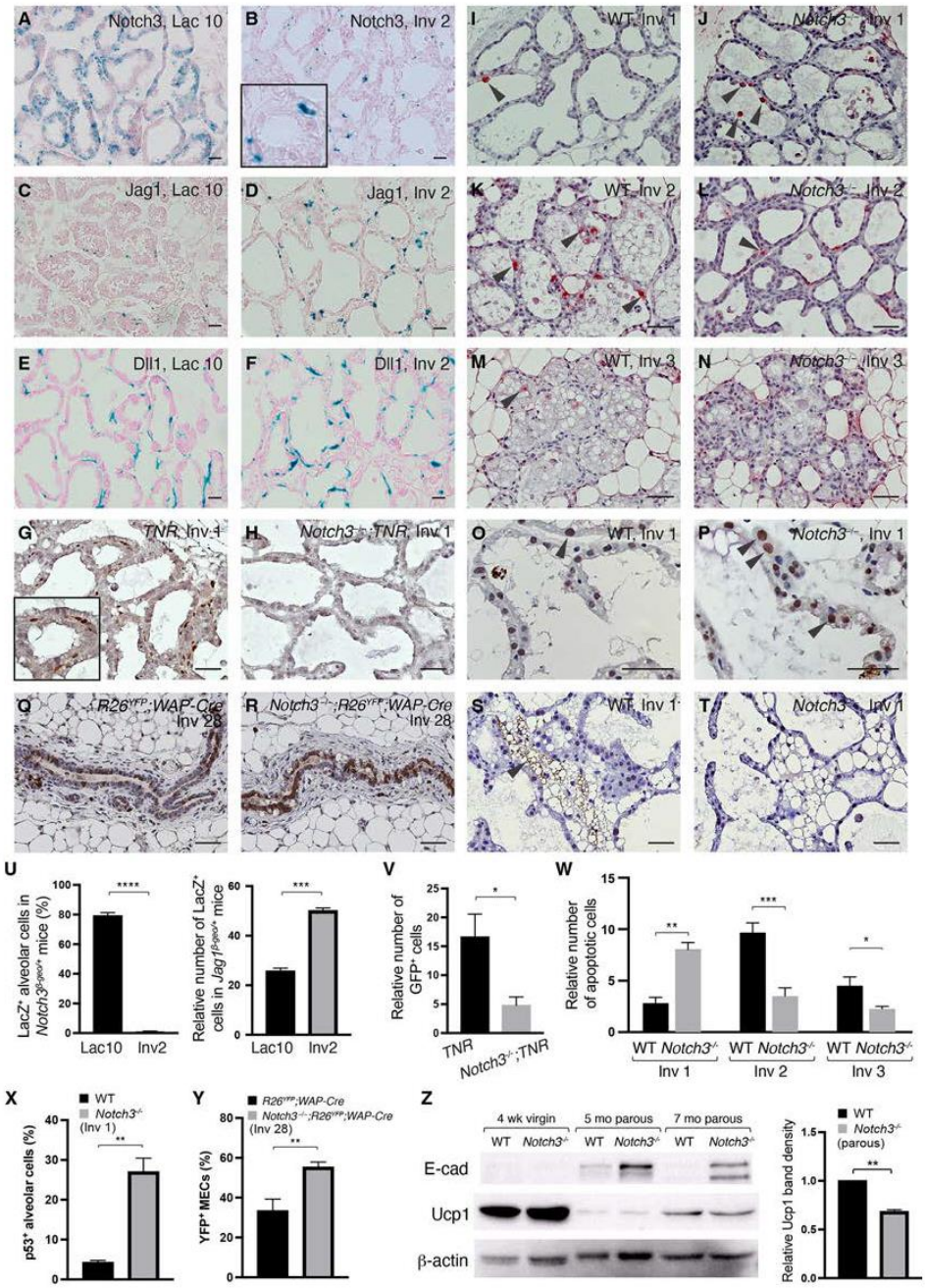

Fig. 2. Decreased Notch activity in myoepithelial cells, altered apoptosis and defective brown adipocyte differentiation during involution, leading to increased PI-MECs in *Notch3*$^{-/-}$ mammary glands. (A-F) X-Gal staining of mammary tissues from *Notch3*$^{β\text{-}geo/+}$, *Jag1*$^{β\text{-}geo/+}$, and *Dll1*$^{lacZ/+}$ mice at lactation day 10 and involution day 2. (G,H) Anti-GFP immunostaining in the mammary tissues of *TNR* and *Notch3*$^{-/-}$*;TNR* mice at involution day 1. Insets in B and G are higher magnifications. (I-N) Representative photomicrographs of TUNEL assays in the mammary tissues of wild-type (WT) and *Notch3*$^{-/-}$ mice at involution days 1, 2 and 3. (O,P) Anti-p53 immunostaining in mammary tissues of wild-type and *Notch3*$^{-/-}$ mice at involution day 1. (Q,R) Anti-YFP immunostaining in mammary tissues from *R26*^{YFP}*;WAP-Cre* and *Notch3*$^{-/-}$*;R26*^{YFP}*;WAP-Cre* mice at involution day 28. (S,T) Immunostaining for Ucp1 in the wild-type and *Notch3*$^{-/-}$ mice at involution day 1. Arrowheads indicate positive staining. (U) Percentage of *lacZ*$^{+}$ alveolar cells in *Notch3*$^{β\text{-}Geo/+}$ mice and relative number of *lacZ*$^{+}$ cells in *Jag1*$^{β\text{-}Geo/+}$ mice at lactation day 10 and involution day 2. (V) Relative number of GFP^{+} cells in *TNR* and *Notch3*$^{-/-}$*;TNR* mice at involution day 1. (W) Quantitation of TUNEL positive cells. (X) Percentage of p53^{+} alveolar cells in the wild-type and *Notch3*$^{-/-}$ mice at involution day 1. (Y) Quantitation of YFP-positive mammary epithelial cells in *R26*^{YFP}*;WAP-Cre* and *Notch3*$^{-/-}$*;R26*^{YFP}*;WAP-Cre* mice at involution day 28. (Z) Western blot analysis of E-cadherin and Ucp1 in mammary tissues from wild-type and *Notch3*$^{-/-}$ mice, and relative levels of Ucp1 normalized with the level of β-actin in parous animals. Scale bars: 50 µm. Data are mean±s.e.m. *P<0.05, **P<0.01, ***P<0.001, ****P<0.0001 (unpaired two-tailed Student's *t*-test).

Development (2022) 149, dev200913. doi:10.1242/dev.200913

epithelial cells at the start of involution in wild-type gland but not in *Notch3*$^{-/-}$ mice (Fig. 2S,T). Brown fat and Ucp1 expression in the mammary gland were previously reported to be highest during prepuberty, decreased upon puberty and almost undetectable in the adult gland (Gouon-Evans and Pollard, 2002). We noted a rapid decrease in Ucp1 staining following the initial stage of involution (data not shown). However, using western blot, Ucp1 expression was still detectable in the mammary gland 3 months after completion of post-lactational involution. In this context, parous *Notch3*$^{-/-}$ mice exhibited lower levels of Ucp1 than their wild-type counterparts (Fig. 2Z). Taken together, deletion of Notch3 led to excess PI-MECs accumulation with an accompanying decrease in brown adipocytes.

Parous Notch3 null mice show mammary hyperplasia with mammary tumor formation

Given expansion of the PI-MEC compartment in postpartum Notch3 mutant mice, we tested for mammary tumor development in these mice. Using whole-mount analysis, mammary glands from parous *Notch3*$^{-/-}$ mutants older than 10 months of age showed severe hyperplasia (n=12). In contrast, few parous mammary glands from wild-type or *Notch3*$^{+/-}$ mice of the same age showed hyperplasia (Fig. 3A,B). In agreement with mammary epithelial hyperplasia, *Notch3* mutant glands showed drastically elevated levels of E-cadherin compared with wild-type mice (Fig. 2Z). In addition, *Notch3* mutant glands exhibited expansion of the lobule progenitor-enriched CD24^{hi}CD49f^{lo} population (Fig. 3C). Multiparous *Notch3*$^{-/-}$ mice of advanced age developed tumorous lesions arising from hyperplastic alveoli or from inside dilated ducts. Some of these progressed to invasive mammary tumors, whereas age-matched nulliparous *Notch3*$^{-/-}$ mice were hyperplasia and tumor free (Fig. 3D). Among animals under tumor watch, 10 out of 33 parous *Notch3*$^{-/-}$ mice, 0 out of 13 nulliparous *Notch3*$^{-/-}$ mice and 0 out of 37 parous controls (including wild type and *Notch3*$^{+/-}$) developed full-blown mammary tumors (Fig. 3E). Of note, 3 out of 10 *Notch3*$^{-/-}$ mice that developed mammary tumors showed metastasis to the lung (see below, Fig. 4U-Y). Interestingly, X-gal staining was seen in benign tissues and in tumor-associated stroma from *Notch3*$^{\beta\text{-}geo/\beta\text{-}geo}$ glands, but not within tumor cells (Fig. 3F). We also used flow cytometry to compare tumor-free mammary glands with tumors isolated from *Notch3*$^{-/-}$ mice, and found that >70% of tumor cells were CD24^{hi}CD49f^{lo} compared with ∼20% in epithelial cells in tumor-free glands (Fig. 3G). These data suggest that loss of Notch3 caused inhibition of luminal/alveolar differentiation and accumulation of lobule progenitors (CD24^{hi}CD49f^{lo}) in the parous gland, ultimately leading to malignant transformation of these cells.

Mammary tumors in Notch3 deletion mice exhibit luminal characteristics

Histological analysis of mammary tumors in *Notch3*$^{-/-}$ mice identified solid sheets of neoplastic cells (Fig. 4A), as well as glandular (Fig. 4B) and papillary (Fig. 4C) patterns with occasional squamous differentiation (Fig. 4D). The majority (6/9) of *Notch3*$^{-/-}$ mammary tumors were estrogen receptor (ER)-positive (Fig. 4E-H). Given that deletion of Notch3 caused expansion of PI-MECs and that cyclin D1 activity was shown to be required for PI-MEC self-renewal and activity (Jeselsohn et al., 2010), we speculated that cyclin D1 may be essential in these tumors. Indeed, all *Notch3*$^{-/-}$ mammary tumors showed high level of cyclin D1 expression (Fig. 4I-L). Also, the vast majority of *Notch3*$^{-/-}$ mammary tumor cells stained positive for the luminal marker keratin 8, with a small subset showing co-expression of keratin 8 and keratin 14, a basal marker (Fig. 4M-O). In a few tumors, almost all cells co-expressed keratin 8 and keratin 14 (Fig. 4P-R), suggesting that such tumors may have originated from a bipotent progenitor. Tumors with squamous differentiation stained positive for keratin 10 as well as for EGFR, which is expressed in human breast tumors with squamous differentiation (Bossuyt et al., 2005) (Fig. 4S,T). As with primary tumors, lung metastasis in these mice stained positive for keratin 8, with a small subset of cells expressing keratin 14. Consistent with the mammary tumor origin of these lesions, these lesions did not express surfactant protein C (SPC), a marker for lung adenocarcinoma (Fig. 4W-Y). Thus, loss of Notch3 induced luminal subtype mammary tumors with the potential for metastatic dissemination to the lung.

Expression from the *Notch3* locus is repressed by Wnt signaling through β-catenin binding and maintenance of a repressed chromatin state. This effect functions as part of Wnt-mediated suppression of luminal/alveolar differentiation in MaSC-enriched basal cells (Gu et al., 2013). In agreement with previous findings, X-gal staining was not seen in tumor cells nor in benign mammary ductal cells from *Notch3*$^{\beta\text{-}geo/+}$*;MMTV-Wnt1* mice (Fig. S3A). Deletion of Notch3 had no effect on Wnt-induced mammary tumor development (Fig. S3B), further supporting the idea that repression of Notch3 occurs downstream of Wnt activation. Although both have lost Notch3 expression, mammary tumors in *Notch3*$^{-/-}$ mice have a luminal phenotype, whereas *MMTV-Wnt1* lesions are mostly keratin 14^{+} cells (Fig. S3C). Different tumor phenotypes may be attributed to distinct cells-of-origin. *MMTV-Wnt1* tumors are thought to originate from CD24^{med}CD49f^{hi} ductal progenitors (Jeselsohn et al., 2010), whereas *Notch3*$^{-/-}$ tumors likely arise through transformation of CD24^{hi}CD49f^{lo} lobule progenitors.

The postpartum microenvironment is required for repopulating activity of mammary epithelial cells isolated from parous *Notch3*$^{-/-}$ mice

The microenvironment is emerging as an important regulator of MaSC (Fu et al., 2020), and the postpartum mammary gland microenvironment has been shown to mediate breast cancer progression (Schedin et al., 2007). For this reason, we tested whether postpartum stroma plays a role in regulation of mammary epithelial specification from PI-MECs. Specifically, we injected mammary epithelial cells from parous *Notch3*$^{\beta\text{-}geo/\beta\text{-}geo}$ mice into mammary fat pads of nulliparous wild-type mice or age-matched wild-type mice at involution day 21 (all on an FVB background). Whole-mount X-gal staining at 8 weeks post-injection showed incorporation of *Notch3*$^{\beta\text{-}geo/\beta\text{-}geo}$ PI-MECs into mammary glands of the postpartum but not nulliparous host mice (in three independent experiments) (Fig. 5A,B). Interestingly, the vast majority of X-gal^{+} cells were found in alveolar buds, indicating that *Notch3*$^{\beta\text{-}geo/\beta\text{-}geo}$ PI-MECs contribute primarily to these structures. Alveolar buds in the mouse mammary glands are somewhat related to terminal ductal lobular units in humans, the primary anatomical source of most breast cancers. For comparison, both nulliparous and parous (3 months post-weaning) *Notch3*$^{\beta\text{-}geo/\beta\text{-}geo}$ mice showed X-gal staining throughout mammary ducts (Fig. 5C), and Notch3 protein levels were similar in age-matched nulliparous and parous wild-type mice (Fig. 5D), indicating that parity does not alter Notch3 expression in the mammary gland. Thus, negative X-gal staining in the *Notch3*$^{\beta\text{-}geo/\beta\text{-}geo}$ cell-injected nulliparous hosts is most likely due to failed incorporation of injected cells into the host glands, rather than silencing of the *Notch3* locus in the nulliparous microenvironment. These results suggest that

Development (2022) 149, dev200913. doi:10.1242/dev.200913

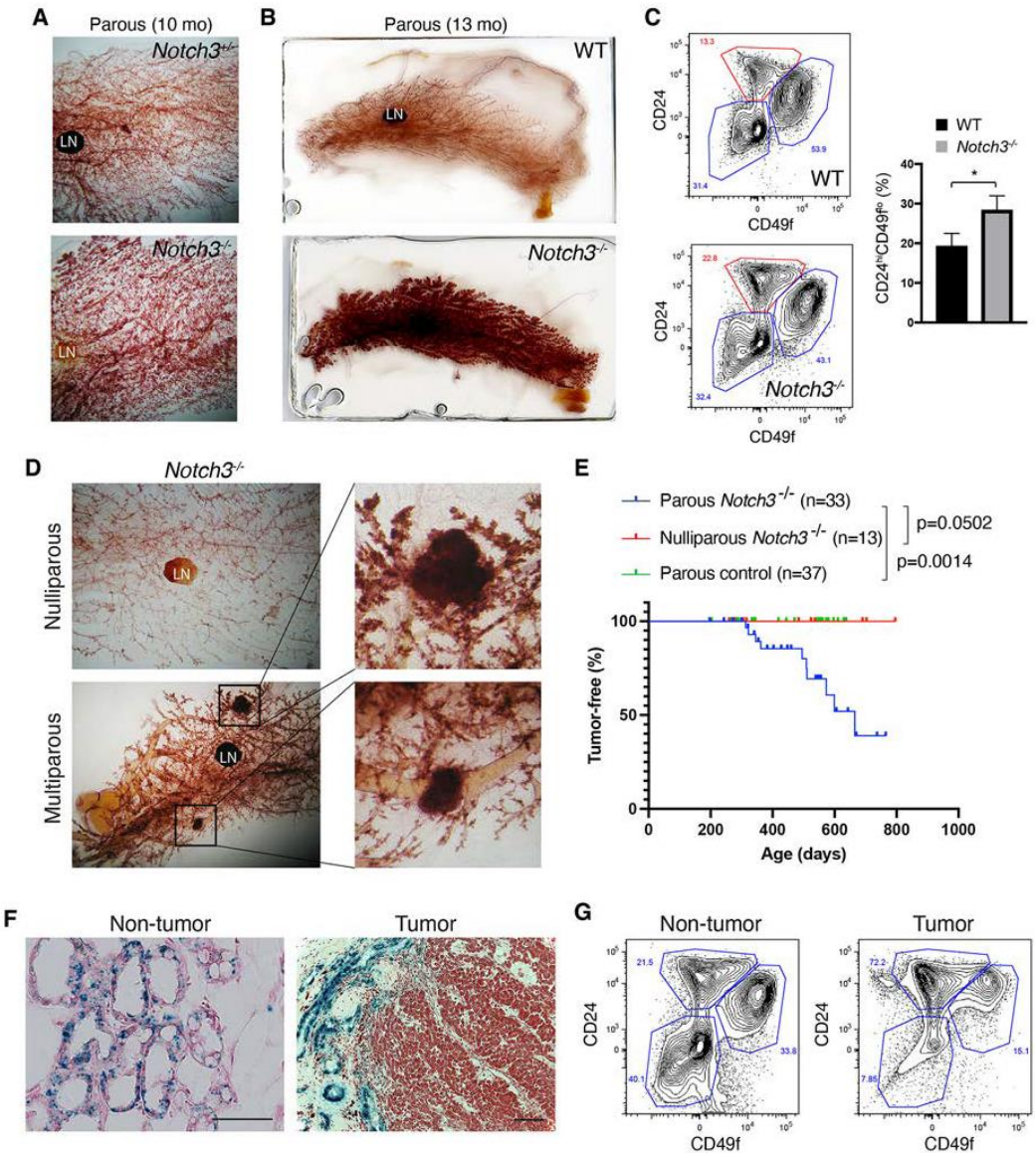

Fig. 3. Mammary hyperplasia and tumor development in parous *Notch3*$^{-/-}$ mice. (A) Whole-mount mammary glands from 10-month-old parous *Notch3*$^{+/-}$ and *Notch3*$^{-/-}$ littermates. (B) Whole-mount mammary glands of parous wild-type (WT) and *Notch3*$^{-/-}$ mice at 13 months of age. (C) CD24/CD49f flow cytometry analysis and quantitation of CD24^{hi}CD49f^{lo} cells among linage-depleted mammary cells from 8-month-old parous wild-type and *Notch3*$^{-/-}$ mice. (D) Representative photomicrographs of whole-mount mammary glands from nulliparous and multiparous *Notch3*$^{-/-}$ mice at 14-16 months of age. Panels on right show magnification of boxed areas in bottom left panel. (E) Kaplan–Meier mammary tumor-free survival curve for parous and nulliparous *Notch3*$^{-/-}$ mice and parous control (wild type and *Notch3*$^{+/-}$) mice. (F) X-Gal staining of non-tumorous mammary tissue and mammary tumor from a *Notch3*$^{β\text{-}geo/β\text{-}geo}$ mouse. (G) Representative CD24/CD49f flow cytometry analysis in linage-depleted non-tumorous mammary cells and tumor cells from parous *Notch3*$^{-/-}$ mice. Scale bars: 50 µm. LN, lymph node. Data are mean±s.e.m. *P<0.05 (paired two-tailed Student's t-test).

postpartum microenvironment may affect PI-MEC stem cell activity.

High NOTCH3 expression is associated with better survival in patients with luminal subtype breast cancer

As deletion of Notch3 caused hyperplasia and luminal-like mammary tumors in multiparous mice, we analyzed *NOTCH3* expression in human breast cancer. Survival analysis using publicly available patient data revealed a significant association between high level *NOTCH3* gene expression and prolonged relapse-free survival in luminal A, luminal B and HER2-positive tumors, but not in basal-like disease. High *NOTCH3* expression also correlates with better overall survival in luminal A subtype (Fig. 6A). As noted above, postpartum microenvironment is required for stem cell activity of *Notch3*$^{-/-}$ PI-MECs. Notch3 mutants had decreased brown adipocytes during post-lactational involution and lower Ucp1 expression compared with wild-type mice. Interestingly, UCP1 was recently found to inhibit tumor

Development (2022) 149, dev200913. doi:10.1242/dev.200913

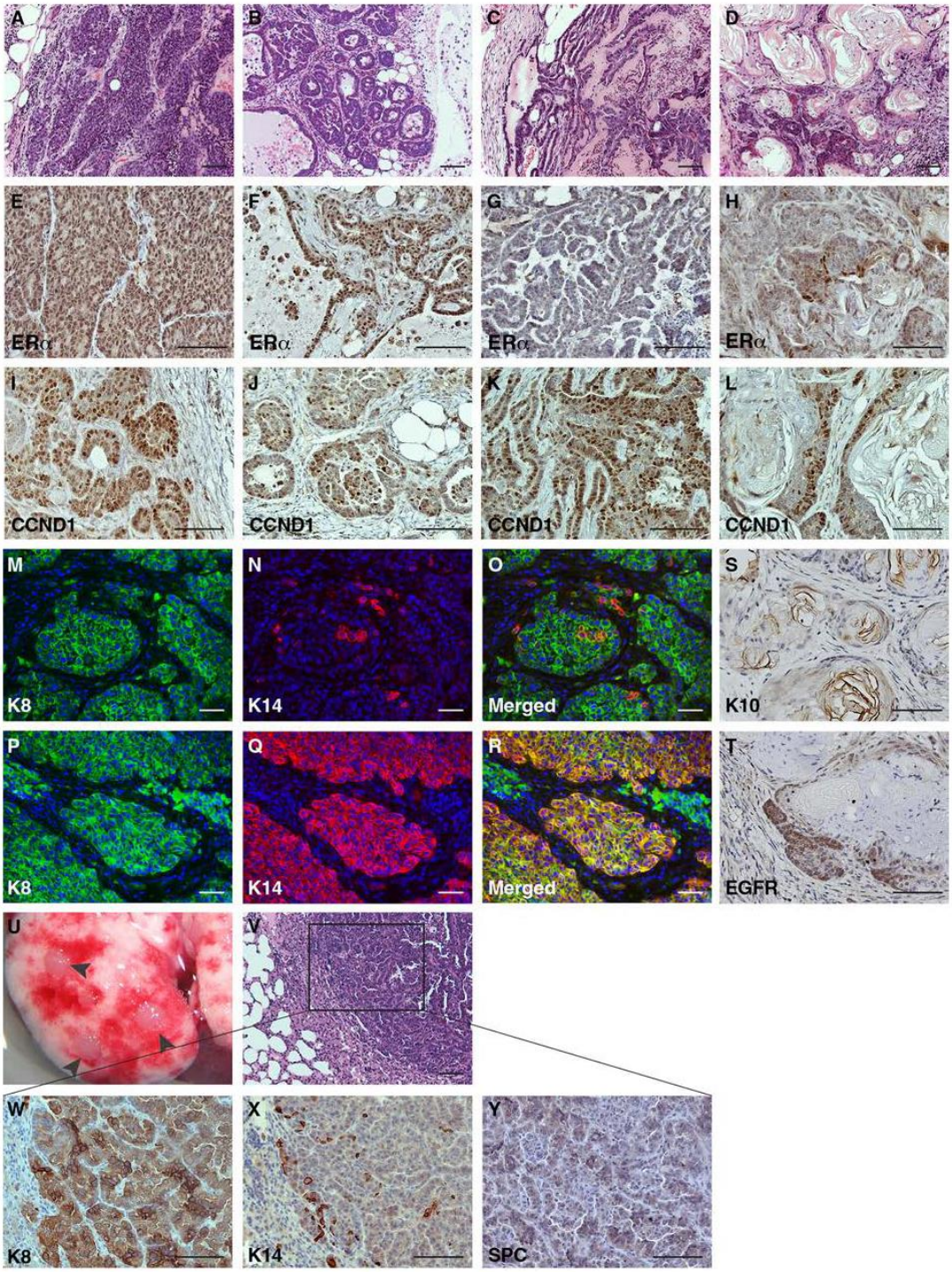

Fig. 4. Histological and immunohistochemical analyses of mammary tumors in parous *Notch3*$^{-/-}$ mice. (A-D) Representative histology of *Notch3*$^{-/-}$ mammary tumors showing solid sheets (A), glandular (B) and papillary (C) patterns, and squamous differentiation (D). (E-H) Immunostaining for ERα in *Notch3*$^{-/-}$ mammary tumors. (I-L) Immunostaining for cyclin D1 (CCND1) in *Notch3*$^{-/-}$ mammary tumors. (M-R) Immunofluorescence staining for keratin 8 (K8) and keratin 14 (K14) in *Notch3*$^{-/-}$ mammary tumors. (S,T) Immunostaining for K10 and EGFR in *Notch3*$^{-/-}$ mammary tumors with squamous differentiation. (U) Gross pathology of the lung with metastasis (arrowheads). (V) Histology of the tumor metastasized to the lung. (W-Y) Immunostaining for K8, K14 and SPC in lung metastasis (boxed area in V). Scale bars: 50 µm.

Development (2022) 149, dev200913. doi:10.1242/dev.200913

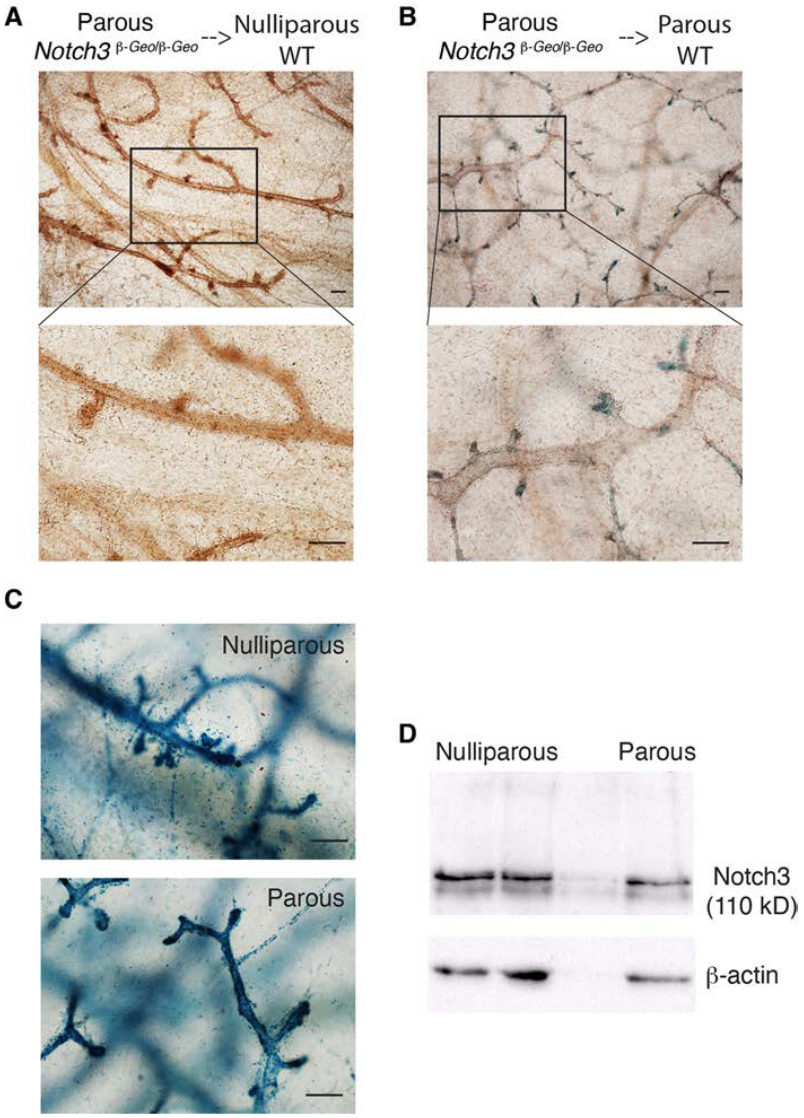

Fig. 5. The postpartum microenvironment is required for stem cell activity of mammary epithelial cells isolated from parous *Notch3*$^{-/-}$ mice. (A) Whole-mount X-gal staining of a nulliparous wild-type (WT) mammary gland harvested at 8 weeks post transplantation of mammary epithelial cells isolated from a parous *Notch3*$^{β\text{-}Geo/β\text{-}Geo}$ donor. (B) Whole-mount X-gal staining of a parous wild-type mammary gland 8 weeks after injection of parous *Notch3*$^{β\text{-}Geo/β\text{-}Geo}$ mammary epithelial cells at involution day 21. X-Gal staining in A and B were counterstained with Hematoxylin. (C) Whole-mount X-gal staining of mammary glands from nulliparous and parous *Notch3*$^{β\text{-}Geo/β\text{-}Geo}$ mice. (D) Western blot analysis for Notch3 in mammary tissues from age-matched nulliparous and parous wild-type mice. Scale bars: 100 µm.

progression through the suppression of the ALDH-positive breast cancer stem cell population in basal-like breast cancer (Zhang et al., 2020). Therefore, we analyzed UCP1 expression related to patient survival in human breast cancer datasets. Indeed, UCP1 expression was positively related to relapse-free survival in all four subtypes as well as overall survival in luminal A subtype (Fig. 6B). Although patient parity status is unknown, these data suggest that NOTCH3 and UCP1 play an important role in human breast cancer, especially in the luminal subtypes of the disease.

DISCUSSION

Signaling through Notch receptors plays a crucial role in the regulation of the mammary epithelial hierarchy. *Notch3* mRNA expression is highest among Notch receptor genes in the mouse mammary gland (Raafat et al., 2011). Subsequent analysis found that *Notch3* is expressed in a highly clonogenic but quiescent progenitor population that gives rise to luminal cells during mammary gland development. These cells can survive multiple cycles of pregnancy and involution, and Notch3 activation restricts proliferation and clonal expansion of these cells (Lafkas et al., 2013). Interestingly, mice expressing an activated form of Notch3 (MMTV-Notch3^{ICD}) show expansion of premalignant CD24^{+}CD29^{lo} luminal progenitors during pregnancy, ultimately leading to luminal mammary tumors in parous mice (Ling et al., 2013). In this paper, we show that Notch3 expression is predominantly restricted to luminal compartment cells of the mammary gland, throughout development, except briefly during early-stage involution, when it is expressed in basal cells. In agreement with a role for Notch3 in promoting luminal lineage specification (Lafkas et al., 2013; Raouf et al., 2008), we found that deletion of *Notch3* results in decreased number of common luminal progenitors (CD24^{hi}CD49f^{lo}CD61^{+}) at puberty and early alveolar progenitors (CD24^{hi}CD49f^{lo}CD61^{+}Sca1^{-}) at mid-pregnancy.

Development (2022) 149, dev200913. doi:10.1242/dev.200913

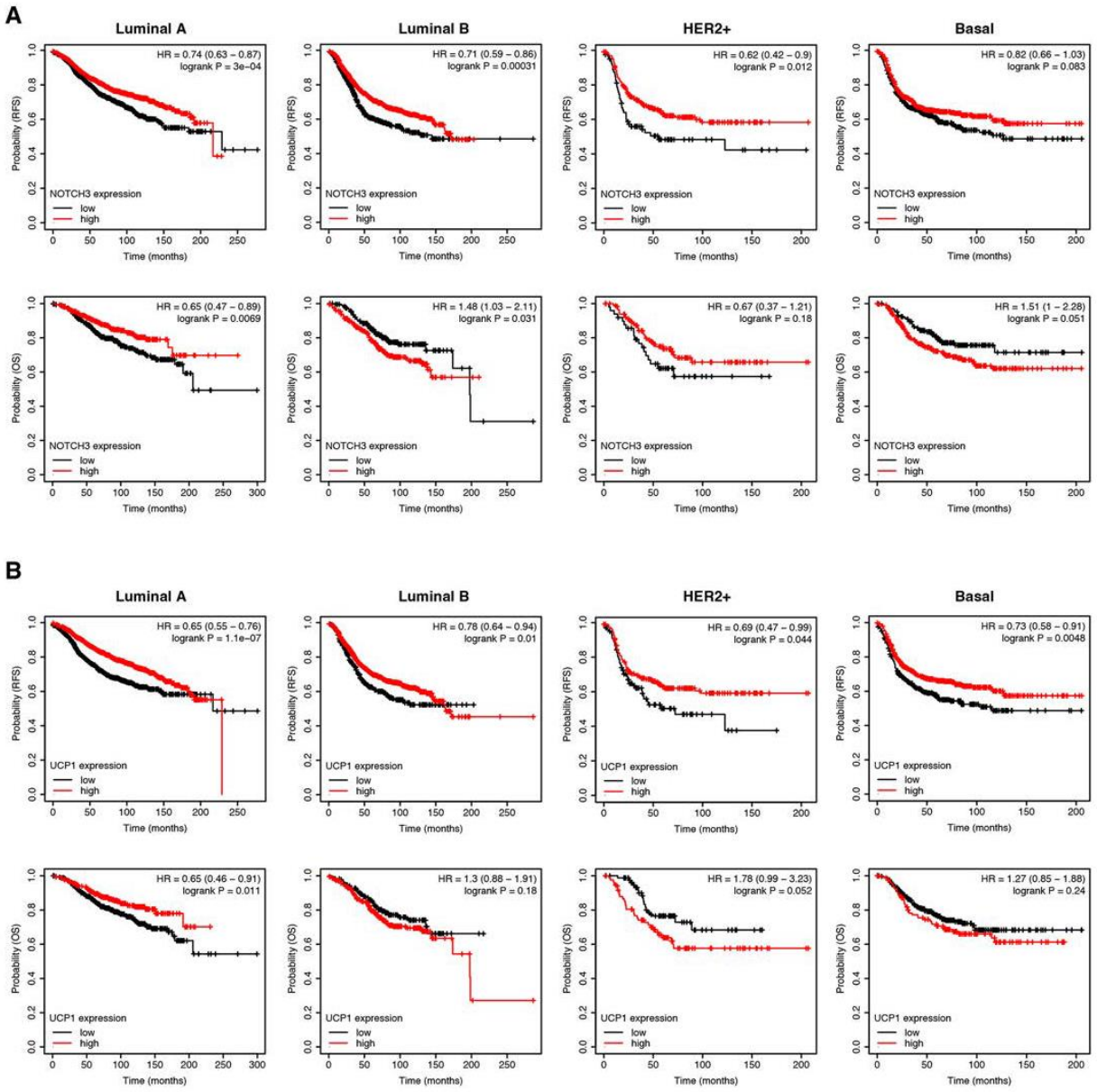

Fig. 6. High expressions of NOTCH3 and UCP1 are associated with prolonged survival in patients with luminal breast cancer. (A) Survival analyses in breast cancer patients using univariate Cox regression and Kaplan–Meier methods. Relapse-free survival rates in patients with high NOTCH3 expression are significantly higher than those in patients with low NOTCH3 expression in all except the basal subtype of breast cancer. Overall survival rate in patients with high NOTCH3 expression is significantly higher than that in patients with low NOTCH3 expression in luminal A subtype. (B) Relapse-free survival rates in patients with high UCP1 expression are significantly higher than those in patients with low UCP1 expression in all breast cancer subtypes. Overall survival rate in patients with high UCP1 is significantly higher than that in patients with low UCP1 in luminal A subtype.

To our surprise, parous *Notch3*$^{-/-}$ mice showed expansion of the CD24^{hi}CD49f^{lo} population, leading to mammary hyperplasia with mammary tumor formation. It appears to be paradoxical that overexpression and loss of Notch3 both result in expansion of luminal progenitors and mammary tumors. Notably, expansion of CD24^{+}CD29^{lo} luminal progenitors started from pregnancy in MMTV-Notch3^{ICD} mice, evidenced by higher bromodeoxyuridine incorporation in these cells (Ling et al., 2013). To the contrary, *Notch3*$^{-/-}$ mice showed decreased alveolar progenitors during pregnancy, and the expansion of the CD24^{hi}CD49f^{lo} population was only observed after the post-lactational involution. CD24^{hi}CD49f^{lo} cells have been shown to enrich for PI-MECs and lobule progenitor cells (Jeselsohn et al., 2010). Lineage tracing of WAP-Cre-labeled cells revealed an increased accumulation of PI-MECs in *Notch3*$^{-/-}$ mice, which may contribute to, at least in part, expansion of CD24^{hi}CD49f^{lo} population in these mice.

Development (2022) 149, dev200913. doi:10.1242/dev.200913

Finally, MMTV-Notch3^{ICD} tumors are negative for keratin 18 and keratin 14 (Ling et al., 2013), whereas *Notch3*$^{-/-}$ tumors express keratin 8, with a subset co-expressing keratin 14, suggesting distinct tumor phenotypes.

Notch3 has previously been associated with the highly aggressive triple-negative breast cancer, including basal-like and claudin-low tumors (Choy et al., 2017; Chung et al., 2017; Turner et al., 2010; Xu et al., 2012). Signaling mediated by IL6 and Notch3 was shown to promote endocrine resistance in metastatic luminal breast cancer through generation of CD133^{hi}/ER^{lo}/IL6^{hi} cancer stem cells (Sansone et al., 2016). However, recent studies suggest that Notch3 maintains a luminal phenotype and may suppress mammary tumorigenesis and metastasis via transactivation of estrogen receptor-α (ERα; *ESR1*) and *PTEN* gene expression (Dou et al., 2017; Zhang et al., 2021). Given the formation of mammary tumors in multiparous but not nulliparous *Notch3*$^{-/-}$ mice, it appears to be clear that Notch3 functions as a tumor suppressor in the postpartum gland. Notably, *Notch3*$^{-/-}$ mammary glands show normal expression of ERα compared with wild-type animals, in both nulliparous and parous contexts (Fig. S4), suggesting that Notch3 does not regulate ERα expression under normal physiological conditions.

Most of the *Notch3*$^{-/-}$ mammary tumors are ERα-positive. The tumor cells express luminal marker keratin 8, with a subset co-expressing the basal marker keratin 14, suggesting a luminal phenotype. In corroboration with our finding that deletion of Notch3 leads to luminal tumors in mice, high *NOTCH3* mRNA expression is associated with better survival in patients with luminal subtype breast cancer. Interestingly, all *Notch3*$^{-/-}$ tumors show high-level expression of cyclin D1. It has been reported that cyclin D1 activity is required for self-renewal of CD24^{hi}CD49f^{lo} mammary stem and progenitor cells in PI-MECs that are targets of MMTV-ErbB2 tumorigenesis (Jeselsohn et al., 2010; Wagner et al., 2013). In light of PI-MEC expansion and CD24^{hi}CD49f^{lo} cell accumulation in parous *Notch3*$^{-/-}$ mice, PI-MECs may also serve as the cell-of-origin in loss-of-Notch3-induced mammary tumorigenesis.

In concert with the switch in Notch3 expression from luminal to basal cells upon involution, Notch is activated specifically in myoepithelial cells of involuting alveoli. *Notch3*$^{-/-}$ mice show drastically decreased Notch activation in these cells, suggesting a non-redundant function of Notch3 in this context. A recent study reveals that myoepithelial cells do not die concomitantly with the luminal cells during involution; instead, they reorganize into parallel strands of ducts or remain as small outpouchings (Hitchcock et al., 2020). It is tantalizing to speculate that some PI-MECs detected in parous mice may represent myoepithelial cells that survived involution, and loss of Notch3 in these cells may cause decreased apoptosis and/or increased proliferation.

Brown adipocytes may regulate mammary epithelial differentiation (Gouon-Evans and Pollard, 2002). We observed a transient emergence of brown adipocytes in wild-type but not *Notch3*$^{-/-}$ mice during early involution. Mammary alveolar epithelial cells can convert into brown adipocytes in post-lactational mice (Giordano et al., 2017), and myoepithelial cells can be induced to differentiate into beige/brite adipocytes *in vitro* (Li et al., 2017), raising the possibility of Notch3-regulated alveolar myoepithelial cell to brown adipocyte transdifferentiation during involution. Despite this, quantitative lineage tracing showed that less than 1% of brown adipocytes were derived from mammary epithelium in the post-weaning gland (Li et al., 2017). Notch3 was recently identified as the major Notch receptor involved in brown adipogenesis from multipotent mesenchymal cells (Rodríguez-Cano et al., 2020). As *Notch3*$^{β\text{-}geo}$ is likely to represent a null allele, loss-of-function in the stroma should disrupt brown adipocyte differentiation. Intriguingly, breast cancer cells co-cultured with Ucp1-deficient adipocytes showed an increased proportion of cancer stem cells, suggesting a potential tumor-suppressive role for Ucp1 in the tumor microenvironment (Zhang et al., 2020). Indeed, like NOTCH3, high expression of UCP1 is associated with prolonged relapse-free survival, especially in patients with luminal subtype tumors.

Finally, transplantation of parous *Notch3*$^{-/-}$ mammary epithelial cells into the mammary fat pad of wild-type mice showed that mutant cells were able to incorporate into alveolar buds in parous but not in age-matched nulliparous hosts, indicating a requirement of postpartum microenvironment for clonal activity of *Notch3*$^{-/-}$ PI-MECs. Mammary gland-associated adipocytes were shown to be required for proper epithelial remodeling and differentiation during involution (Zwick et al., 2018). Other components of the parous gland microenvironment, including immune cells, fibroblasts, and blood and lymphatic vasculatures, may also control PI-MEC cell behavior, and thereby regulate mammary tumorigenesis.

MATERIALS AND METHODS

Mice

Generation of the *Notch3*$^{β\text{-}geo}$ mouse strain has been previously described (Xu et al., 2010). TNR mice (Duncan et al., 2005) were kindly provided by Dr Nicholas Gaiano (Johns Hopkins University School of Medicine, Baltimore, MD, USA). R26YFP, WAP-Cre and MMTV-Wnt1 were purchased from the Jackson Laboratory. Mice were housed under standard condition and all mouse procedures were performed in accordance with protocols approved by Institutional Animal Care and Use Committees at the University of Mississippi Medical Center and the Hospital for Sick Children.

Mammary gland whole-mount preparation, morphometric analysis and X-gal staining

All analyses were performed using number four (inguinal) mammary glands. Whole-mount mammary glands were stained with Hematoxylin according to standard procedure. Morphometric analysis was performed using ImageJ software. The length of ductal elongation was assessed by measuring the mean distance from nipple to the three most distal TEBs in each mammary gland. The density of branch points was the mean number of branch points on the three longest primary ducts divided by their mean length. For the size of alveoli (area), at least ten representative alveoli in each gland were measured to calculate the mean value. The mean size of alveoli is compared between three pairs of wild-type and *Notch3*$^{-/-}$ littermates, and presented as fold change. For X-gal staining, mammary tissues were fixed in 1.0% formaldehyde and 0.02% Nonidet P-40 (in PBS) overnight, and stained with X-gal between 4 and 16 h. X-gal staining of frozen sections was counterstained with 0.5% Eosin. Some of the whole-mount X-gal staining was counterstained with Hematoxylin, or paraffin-embedded for sectioning and counterstaining with Neutral-red.

Histology and immunohistochemistry

Formalin-fixed paraffin-embedded mouse mammary tissues were processed for Hematoxylin and Eosin staining by standard procedure. For immunostaining, 5 µm sections were rehydrated, processed by microwave antigen retrieval and stained according to standard protocol. Representative photomicrographs were acquired using a Nikon Eclipse 80i microscope. Primary antibodies used for immunostaining were: GFP (Abcam, ab6673, 1:200), Cytokeratin 8 (Fitzgerald, 10R-C177AX, 1:10), Cytokeratin 14 (Panomics, E2624, 1:200), YFP (Invitrogen, A-11122, 1:200), Ucp1 (ProteinTech, 23673-1-AP, 1:200), ERα (Santa Cruz Biotechnology, sc-542, 1:200), Cyclin D1 (Santa Cruz Biotechnology, sc-753, 1:200), Cytokeratin 10 (Santa Cruz Biotechnology, sc-23877, 1:200), EGFR (Abcam, ab32077, 1:200) and SPC (Santa Cruz Biotechnology, sc-13979, 1:200).

Western blot analysis

Mammary tissues were homogenized and lysed in RIPA buffer (Boston BioProducts) supplemented with protease inhibitor (Roche). Supernatants were clarified by centrifugation (20,000 *g*), and total amount of proteins were quantified. Equivalent amounts of proteins from each sample were loaded for western blots, performed according to standard methodology. Antibodies for probing specified proteins are as follows: E-cadherin (Cell Signaling Technology, 3195, 1:1000), Ucp1 (ProteinTech, 23673-1-AP, 1:1000), Notch3 (ProteinTech, 55114-1-AP, 1:1000), and β-Actin (Santa Cruz Biotechnology, sc-81178, 1:5000).

Flow cytometry

Mouse mammary tissues were dissociated in Collagenase/Hyaluronidase solution (StemCell Technologies) and prepared for single cell suspensions. Lineage-depleted mammary epithelial cells were generated using EasySep mouse mammary stem cell enrichment kit (StemCell Technologies) according to the manufacturer's instructions. Flow cytometry of lineage-depleted cells was performed using a BD LSR-II Flow Cytometer (BD Biosciences) as per the manufacturer's protocol with the following antibodies: PE-Cy5 rat anti-human CD49f (BD Pharmingen, 551129, 1:500), PE-Cy7 anti-mouse Ly-6A/E (Sca-1) (eBioscience, 25-5981, 1:500), eFluor 450 anti-mouse CD24 (eBioscience, 48-0242, 1:400) and R-PE hamster anti-mouse/rat CD61 (Invitrogen, MCD6104, 1:400). Fluorescence was recorded using BD LSR-II flow cytometer and analyzed with FlowJo 9.1 (Treestar). Dead cells were excluded based on propidium iodide staining. Mammary tissues from three animals per genotype were analyzed with similar results.

Mammary epithelial cell transplantation

Lineage-depleted mammary epithelial cells were prepared from parous *Notch3*$^{\beta\text{-}geo/\beta\text{-}geo}$ mice (having been backcrossed to FVB for at least six generations). Approximately 2×10^5 lineage-depleted cells were resuspended in DMEM medium and mixed at 1:1 ratio with 20 µl Matrigel (BD Bioscience) on ice. A total of 40 µl cell sample was then injected into each of the inguinal mammary gland in syngeneic FVB mice at involution day 21 or age-matched nulliparous FVB mice, under anesthesia with isoflurane. Host mammary glands were harvested for analysis at 8 weeks after transplantation.

Gene expression analysis of human data sets

For the survival analysis related to NOTCH3 (203238_s_at) and UCP1 (221384_at) expressions, we used online tool (https://kmplot.com/analysis/) to perform univariate Cox regression analysis and Kaplan–Meier survival curves. The breast cancer database on this site was set up by downloading transcriptome-level gene expression datasets with available clinical information from the GEO (https://www.ncbi.nlm.nih.gov/geo/) and EGA (https://ega-archive.org/) repositories. Only datasets with at least 30 samples and only those which were generated using the GEO platforms GPL96, GPL570 and GPL571 were included (Győrffy, 2021). The high versus low gene expression was determined using best cut-off (Lánczky and Győrffy, 2021). The hazard ratio with 95% confidence and *P*-values were calculated from 846 patients with basal subtype of breast cancer, 2277 patients with luminal A subtype, 1491 patients with luminal B subtype, and 315 patients with HER2$^+$ subtype that have relapse-free survival information, and from 404 patients with basal subtype, 794 patients with luminal A subtype, 515 patients with luminal B subtype and 166 patients with HER2$^+$ subtype having overall survival information.

Statistics

Statistical analyses were performed using Prism version 9.2.0 (GraphPad Software). All data are presented as the mean with standard error of the mean (s.e.m.). Two-group comparisons were analyzed using two-tailed Student's *t*-test. Mouse tumor-free survival was calculated by the Kaplan–Meier method and compared using nonparametric log-rank test. *P*-value of 0.05 or less was considered statistically significant.

Acknowledgements

The authors thank Dr Nicholas Gaiano for providing us with *TNR* mice and Dr Robert D. Cardiff for the pathological evaluation of mouse mammary tumors.

Competing interests

The authors declare no competing or financial interests.

Author contributions

Conceptualization: S.E.E., K.X.; Methodology: W.-C.C.; Validation: W.-C.C., S.E.E., K.X.; Formal analysis: W.-C.C., K.X.; Investigation: W.-C.C., K.X.; Resources: S.E.E., K.X.; Data curation: W.-C.C.; Writing - original draft: K.X.; Writing - review & editing: W.-C.C., S.E.E., K.X.; Supervision: S.E.E., K.X.; Project administration: K.X.; Funding acquisition: S.E.E., K.X.

Funding

This work was supported by a U.S. Department of Defense grant W81XWH-19-1-0031 to K.X. and a grant from the Canadian Cancer Society Research Institute to S.E.E.

Peer review history

The peer review history is available online at https://journals.biologists.com/dev/lookup/doi/10.1242/dev.200913.reviewer-comments.pdf

References

Albrektsen, G., Heuch, I., Hansen, S. and Kvåle, G. (2005). Breast cancer risk by age at birth, time since birth and time intervals between births: exploring interaction effects. *Br. J. Cancer* **92**, 167-175. doi:10.1038/sj.bjc.6602302

Asselin-Labat, M. L., Sutherland, K. D., Barker, H., Thomas, R., Shackleton, M., Forrest, N. C., Hartley, L., Robb, L., Grosveld, F. G., van der Wees, J. et al. (2007). Gata-3 is an essential regulator of mammary-gland morphogenesis and luminal-cell differentiation. *Nat. Cell Biol.* **9**, 201-209. doi:10.1038/ncb1530

Asselin-Labat, M. L., Vaillant, F., Sheridan, J. M., Pal, B., Wu, D., Simpson, E. R., Yasuda, H., Smyth, G. K., Martin, T. J., Lindeman, G. J. et al. (2010). Control of mammary stem cell function by steroid hormone signalling. *Nature* **465**, 798-802. doi:10.1038/nature09027

Bossuyt, V., Fadare, O., Martel, M., Ocal, I. T., Burtness, B., Moinfar, F., Leibl, S. and Tavassoli, F. A. (2005). Remarkably high frequency of EGFR expression in breast carcinomas with squamous differentiation. *Int. J. Surg. Pathol.* **13**, 319-327. doi:10.1177/106689690501300403

Boulanger, C. A., Wagner, K. U. and Smith, G. H. (2005). Parity-induced mouse mammary epithelial cells are pluripotent, self-renewing and sensitive to TGF-β1 expression. *Oncogene* **24**, 552-560. doi:10.1038/sj.onc.1208185

Chie, W.-C., Hsieh, C., Newcomb, P. A., Longnecker, M. P., Mittendorf, R., Greenberg, E. R., Clapp, R. W., Burke, K. P., Titus-Ernstoff, L., Trentham-Dietz, A. et al. (2000). Age at any full-term pregnancy and breast cancer risk. *Am. J. Epidemiol.* **151**, 715-722. doi:10.1093/oxfordjournals.aje.a010266

Choy, L., Hagenbeek, T. J., Solon, M., French, D., Finkle, D., Shelton, A., Venook, R., Brauer, M. J. and Siebel, C. W. (2017). Constitutive NOTCH3 signaling promotes the growth of basal breast cancers. *Cancer Res.* **77**, 1439-1452. doi:10.1158/0008-5472.CAN-16-1022

Chung, W. C., Zhang, S., Challagundla, L., Zhou, Y. and Xu, K. (2017). Lunatic fringe and p53 cooperatively suppress mesenchymal stem-like breast cancer. *Neoplasia* **19**, 885-895. doi:10.1016/j.neo.2017.08.006

Dou, X.-W., Liang, Y.-K., Lin, H.-Y., Wei, X.-L., Zhang, Y.-Q., Bai, J.-W., Chen, C.-F., Chen, M., Du, C.-W., Li, Y.-C. et al. (2017). Notch3 maintains luminal phenotype and suppresses tumorigenesis and metastasis of breast cancer via trans-activating estrogen receptor-alpha. *Theranostics* **7**, 4041-4056. doi:10.7150/thno.19989

Duncan, A. W., Rattis, F. M., DiMascio, L. N., Congdon, K. L., Pazianos, G., Zhao, C., Yoon, K., Cook, J. M., Willert, K., Gaiano, N. et al. (2005). Integration of Notch and Wnt signaling in hematopoietic stem cell maintenance. *Nat. Immunol.* **6**, 314-322. doi:10.1038/ni1164

Fu, N. Y., Nolan, E., Lindeman, G. J. and Visvader, J. E. (2020). Stem cells and the differentiation hierarchy in mammary gland development. *Physiol. Rev.* **100**, 489-523. doi:10.1152/physrev.00040.2018

Giordano, A., Perugini, J., Kristensen, D. M., Sartini, L., Frontini, A., Kajimura, S., Kristiansen, K. and Cinti, S. (2017). Mammary alveolar epithelial cells convert to brown adipocytes in post-lactating mice. *J. Cell. Physiol.* **232**, 2923-2928. doi:10.1002/jcp.25858

Gouon-Evans, V. and Pollard, J. W. (2002). Unexpected deposition of brown fat in mammary gland during postnatal development. *Mol. Endocrinol.* **16**, 2618-2627. doi:10.1210/me.2001-0337

Gu, B., Watanabe, K., Sun, P., Fallahi, M. and Dai, X. (2013). Chromatin effector Pygo2 mediates Wnt-notch crosstalk to suppress luminal/alveolar potential of mammary stem and basal cells. *Cell Stem Cell* **13**, 48-61. doi:10.1016/j.stem.2013.04.012

Guo, Q., Minnier, J., Burchard, J., Chiotti, K., Spellman, P. and Schedin, P. (2017). Physiologically activated mammary fibroblasts promote postpartum mammary cancer. *JCI Insight* **2**, e89206. doi:10.1172/jci.insight.89206

Győrffy, B. (2021). Survival analysis across the entire transcriptome identifies biomarkers with the highest prognostic power in breast cancer. *Comput. Struct. Biotechnol. J.* **19**, 4101-4109. doi:10.1016/j.csbj.2021.07.014

Henry, M. D., Triplett, A. A., Oh, K. B., Smith, G. H. and Wagner, K. U. (2004). Parity-induced mammary epithelial cells facilitate tumorigenesis in MMTV-neu transgenic mice. *Oncogene* **23**, 6980-6985. doi:10.1038/sj.onc.1207827

Hitchcock, J. R., Hughes, K., Harris, O. B. and Watson, C. J. (2020). Dynamic architectural interplay between leucocytes and mammary epithelial cells. *FEBS J.* **287**, 250-266. doi:10.1111/febs.15126

Jerry, D. J., Kuperwasser, C., Downing, S. R., Pinkas, J., He, C., Dickinson, E., Marconi, S. and Naber, S. P. (1998). Delayed involution of the mammary epithelium in BALB/c-p53null mice. *Oncogene* **17**, 2305-2312. doi:10.1038/sj.onc.1202157

Jeselsohn, R., Brown, N. E., Arendt, L., Klebba, I., Hu, M. G., Kuperwasser, C. and Hinds, P. W. (2010). Cyclin D1 kinase activity is required for the self-renewal of mammary stem and progenitor cells that are targets of MMTV-ErbB2 tumorigenesis. *Cancer Cell* **17**, 65-76. doi:10.1016/j.ccr.2009.11.024

Lafkas, D., Rodilla, V., Huyghe, M., Mourao, L., Kiaris, H. and Fre, S. (2013). Notch3 marks clonogenic mammary luminal progenitor cells in vivo. *J. Cell Biol.* **203**, 47-56. doi:10.1083/jcb.201307046

Lambe, M., Hsieh, C., Trichopoulos, D., Ekbom, A., Pavia, M. and Adami, H. O. (1994). Transient increase in the risk of breast cancer after giving birth. *N. Engl. J. Med.* **331**, 5-9. doi:10.1056/NEJM199407073310102

Lánczky, A. and Győrffy, B. (2021). Web-based survival analysis tool tailored for medical research (KMplot): development and implementation. *J. Med. Internet Res.* **23**, e27633. doi:10.2196/27633

Li, L., Li, B., Li, M., Niu, C., Wang, G., Li, T., Król, E., Jin, W. and Speakman, J. R. (2017). Brown adipocytes can display a mammary basal myoepithelial cell phenotype in vivo. *Mol. Metab.* **6**, 1198-1211. doi:10.1016/j.molmet.2017.07.015

Ling, H., Sylvestre, J. R. and Jolicoeur, P. (2013). Cyclin D1-dependent induction of luminal inflammatory breast tumors by activated notch3. *Cancer Res.* **73**, 5963-5973. doi:10.1158/0008-5472.CAN-13-0409

Liu, Q., Wuu, J., Lambe, M., Hsieh, S. F., Ekbom, A. and Hsieh, C. C. (2002). Transient increase in breast cancer risk after giving birth: postpartum period with the highest risk (Sweden). *Cancer Causes Control* **13**, 299-305. doi:10.1023/A:1015287208222

Lyons, T. R., O'Brien, J., Borges, V. F., Conklin, M. W., Keely, P. J., Eliceiri, K. W., Marusyk, A., Tan, A. C. and Schedin, P. (2011). Postpartum mammary gland involution drives progression of ductal carcinoma in situ through collagen and COX-2. *Nat. Med.* **17**, 1109-1115. doi:10.1038/nm.2416

Lyons, T. R., Borges, V. F., Betts, C. B., Guo, Q., Kapoor, P., Martinson, H. A., Jindal, S. and Schedin, P. (2014). Cyclooxygenase-2-dependent lymphangiogenesis promotes nodal metastasis of postpartum breast cancer. *J. Clin. Invest.* **124**, 3901-3912. doi:10.1172/JCI73777

Martinson, H. A., Jindal, S., Durand-Rougely, C., Borges, V. F. and Schedin, P. (2015). Wound healing-like immune program facilitates postpartum mammary gland involution and tumor progression. *Int. J. Cancer* **136**, 1803-1813. doi:10.1002/ijc.29181

Matulka, L. A., Triplett, A. A. and Wagner, K. U. (2007). Parity-induced mammary epithelial cells are multipotent and express cell surface markers associated with stem cells. *Dev. Biol.* **303**, 29-44. doi:10.1016/j.ydbio.2006.12.017

Polyak, K. (2006). Pregnancy and breast cancer: the other side of the coin. *Cancer Cell* **9**, 151-153. doi:10.1016/j.ccr.2006.02.026

Raafat, A., Goldhar, A. S., Klauzinska, M., Xu, K., Amirjazil, I., McCurdy, D., Lashin, K., Salomon, D., Vonderhaar, B. K., Egan, S. et al. (2011). Expression of Notch receptors, ligands, and target genes during development of the mouse mammary gland. *J. Cell. Physiol.* **226**, 1940-1952. doi:10.1002/jcp.22526

Raouf, A., Zhao, Y., To, K., Stingl, J., Delaney, A., Barbara, M., Iscove, N., Jones, S., McKinney, S., Emerman, J. et al. (2008). Transcriptome analysis of the normal human mammary cell commitment and differentiation process. *Cell Stem Cell* **3**, 109-118. doi:10.1016/j.stem.2008.05.018

Rodríguez-Cano, M. M., González-Gómez, M. J., Sánchez-Solana, B., Monsalve, E. M., Díaz-Guerra, M. M., Laborda, J., Nueda, M. L. and Baladrón, V. (2020). NOTCH receptors and DLK proteins enhance brown adipogenesis in mesenchymal C3H10T1/2 cells. *Cells* **9**, 2032. doi:10.3390/cells9092032

Sansone, P., Ceccarelli, C., Berishaj, M., Chang, Q., Rajasekhar, V. K., Perna, F., Bowman, R. L., Vidone, M., Daly, L., Nnoli, J. et al. (2016). Self-renewal of CD133(hi) cells by IL6/Notch3 signalling regulates endocrine resistance in metastatic breast cancer. *Nat. Commun.* **7**, 10442. doi:10.1038/ncomms10442

Schedin, P., O'Brien, J., Rudolph, M., Stein, T. and Borges, V. (2007). Microenvironment of the involuting mammary gland mediates mammary cancer progression. *J. Mammary Gland Biol. Neoplasia* **12**, 71-82. doi:10.1007/s10911-007-9039-3

Stingl, J., Eirew, P., Ricketson, I., Shackleton, M., Vaillant, F., Choi, D., Li, H. I. and Eaves, C. J. (2006). Purification and unique properties of mammary epithelial stem cells. *Nature* **439**, 993-997. doi:10.1038/nature04496

Strange, R., Li, F., Saurer, S., Burkhardt, A. and Friis, R. R. (1992). Apoptotic cell death and tissue remodelling during mouse mammary gland involution. *Development* **115**, 49-58. doi:10.1242/dev.115.1.49

Turner, N., Lambros, M. B., Horlings, H. M., Pearson, A., Sharpe, R., Natrajan, R., Geyer, F. C., van Kouwenhove, M., Kreike, B., Mackay, A. et al. (2010). Integrative molecular profiling of triple negative breast cancers identifies amplicon drivers and potential therapeutic targets. *Oncogene* **29**, 2013-2023. doi:10.1038/onc.2009.489

Visvader, J. E. and Stingl, J. (2014). Mammary stem cells and the differentiation hierarchy: current status and perspectives. *Genes Dev.* **28**, 1143-1158. doi:10.1101/gad.242511.114

Wagner, K.-U., Boulanger, C. A., Henry, M. D., Sgagias, M., Hennighausen, L. and Smith, G. H. (2002). An adjunct mammary epithelial cell population in parous females: its role in functional adaptation and tissue renewal. *Development* **129**, 1377-1386. doi:10.1242/dev.129.6.1377

Wagner, K.-U., Booth, B. W., Boulanger, C. A. and Smith, G. H. (2013). Multipotent PI-MECs are the true targets of MMTV-neu tumorigenesis. *Oncogene* **32**, 1338. doi:10.1038/onc.2012.452

Xu, K., Nieuwenhuis, E., Cohen, B. L., Wang, W., Canty, A. J., Danska, J. S., Coultas, L., Rossant, J., Wu, M. Y., Piscione, T. D. et al. (2010). Lunatic Fringe-mediated Notch signaling is required for lung alveogenesis. *Am. J. Physiol. Lung Cell. Mol. Physiol.* **298**, L45-L56. doi:10.1152/ajplung.90550.2008

Xu, K., Usary, J., Kousis, P. C., Prat, A., Wang, D. Y., Adams, J. R., Wang, W., Loch, A. J., Deng, T., Zhao, W. et al. (2012). Lunatic fringe deficiency cooperates with the Met/Caveolin gene amplicon to induce basal-like breast cancer. *Cancer Cell* **21**, 626-641. doi:10.1016/j.ccr.2012.03.041

Zhang, F., Liu, B., Deng, Q., Sheng, D., Xu, J., He, X., Zhang, L. and Liu, S. (2020). UCP1 regulates ALDH-positive breast cancer stem cells through releasing the suppression of Snail on FBP1. *Cell Biol. Toxicol.* **37**, 277-291. doi:10.1007/s10565-020-09533-5

Zhang, Y.-Q., Liang, Y.-K., Wu, Y., Chen, M., Chen, W.-L., Li, R.-H., Zeng, Y.-Z., Huang, W.-H., Wu, J.-D., Zeng, D. et al. (2021). Notch3 inhibits cell proliferation and tumorigenesis and predicts better prognosis in breast cancer through transactivating PTEN. *Cell Death Dis.* **12**, 502. doi:10.1038/s41419-021-03735-3

Zwick, R. K., Rudolph, M. C., Shook, B. A., Holtrup, B., Roth, E., Lei, V., Van Keymeulen, A., Seewaldt, V., Kwei, S., Wysolmerski, J. et al. (2018). Adipocyte hypertrophy and lipid dynamics underlie mammary gland remodeling after lactation. *Nat. Commun.* **9**, 3592. doi:10.1038/s41467-018-05911-0

RESEARCH HIGHLIGHT | 12 OCTOBER 2022

Notch3 protects against birth-associated mammary tumours FREE

+ Author and article information

Development (2022) 149 (19): e149_e1905.

Related content

This is a companion to: A tumor-suppressive function for Notch3 in the parous mammary gland

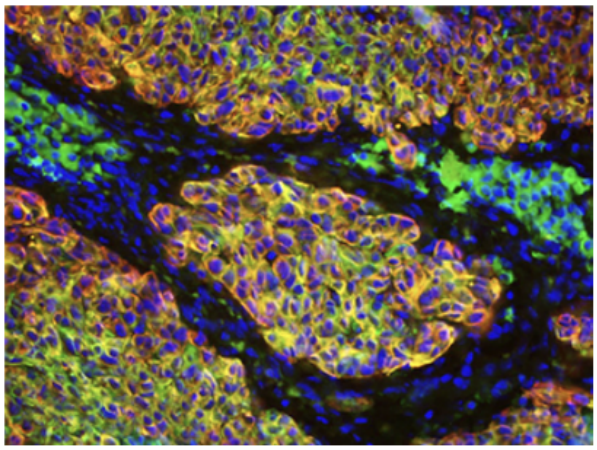

Evidence indicates an increased chance of mammary tumours developing after giving birth and previous studies have shown that the overexpression of Notch3 in mice increases the risk. However, a detailed understanding of Notch3 activity has been lacking. Now, Keli Xu and colleagues employ *Notch3* $^{\beta\text{-geo}}$ mutant mice to define Notch3 loss-of-function phenotypes in mammary epithelium, using immunohistochemistry, flow cytometry and lineage-tracing experiments. They show that *Notch3* deletion reduces the number of luminal or alveolar progenitors during puberty and pregnancy, respectively. Surprisingly, parous mammary glands lacking *Notch3* have an excess of parity-identified mammary epithelial cells (PI-MECs), which arise after birth, as well as increased mammary hyperplasia and luminal-like tumours. The researchers transplanted parous *Notch3*-null PI-MECs into nulliparous (never given birth) or postpartum (just given birth) hosts and found that the transplanted cells only incorporated into postpartum tissue, suggesting that the microenvironment affects PI-MEC activity. Finally, the authors analysed publicly available patient data to show that high levels of Notch3 correlate with relapse-free survival for patients with luminal breast cancer. Although the exact mechanism of Notch3 action needs to be elucidated, these results indicate that Notch3 has a tumour-suppressive function in the parous mammary gland by restricting PI-MEC expansion.